The Journal of Biological Chemistry
AFFINITY SITES
ASBMB
American Society for Biochemistry and Molecular Biology

Glycobiology and Extracellular Matrices:

Decorin Potentiates Interferon-γ Activity in a Model of Allergic Inflammation

Carla Bocian, Ann-Kathrin Urbanowitz, Rick T. Owens, Renato V. Iozzo, Martin Götte and Daniela G. Seidler

J. Biol. Chem. 2013, 288:12699-12711.
doi: 10.1074/jbc.M112.419366 originally published online March 4, 2013

GLYCOBIOLOGY AND EXTRACELLULAR MATRICES
IMMUNOLOGY

Access the most updated version of this article at doi: 10.1074/jbc.M112.419366

Find articles, minireviews, Reflections and Classics on similar topics on the JBC Affinity Sites.

Alerts:
- When this article is cited
- When a correction for this article is posted

Click here to choose from all of JBC's e-mail alerts

Supplemental material:
http://www.jbc.org/content/suppl/2013/03/04/M112.419366.DC1.html

This article cites 67 references, 30 of which can be accessed free at
http://www.jbc.org/content/288/18/12699.full.html#ref-list-1

Downloaded from http://www.jbc.org/ at Istituto Superiore di Sanità on December 12, 2013

THE JOURNAL OF BIOLOGICAL CHEMISTRY VOL. 288, NO. 18, pp. 12699–12711, May 3, 2013
© 2013 by The American Society for Biochemistry and Molecular Biology, Inc. Published in the U.S.A.

Decorin Potentiates Interferon-γ Activity in a Model of Allergic Inflammation*[S]

Received for publication, September 28, 2012, and in revised form, February 15, 2013 Published, JBC Papers in Press, March 4, 2013, DOI 10.1074/jbc.M112.419366

Carla Bocian[‡§], Ann-Kathrin Urbanowitz[‡§], Rick T. Owens[¶], Renato V. Iozzo[‖], Martin Götte[§1], and Daniela G. Seidler[‡1,2]

From the [‡]Institute of Physiological Chemistry and Pathobiochemistry, Waldeyerstrasse 15, 48149 Münster, Germany, the [§]Department of Gynecology and Obstetrics, Münster University Hospital, 48149 Münster, Germany, the [¶]LifeCell Corp., Branchburg, New Jersey 08876, and the [‖]Department of Pathology, Anatomy and Cell Biology, and the Cancer Cell Biology and Signaling Program, Kimmel Cancer Center, Thomas Jefferson University, Philadelphia, Pennsylvania 19107

Background: The dermatan sulfate proteoglycan decorin modulates delayed-type hypersensitivity, leading to reduced edema.
Results: Decorin deficiency leads to a reduced infiltration of CD8$^+$ leukocytes and deregulated cytokine expression. Decorin can stabilize IFN-γ and potentiate its signaling by activating STAT-1.
Conclusion: Decorin is a novel modulator of proallergic signal transduction.
Significance: Decorin is part of a signaling network that regulates cytokine expression in acute inflammation.

The proteoglycan decorin modulates leukocyte recruitment during delayed-type hypersensitivity responses. Decorin-deficient (*Dcn*$^{-/-}$) mice show reduced edema formation during the first 24 h with a concurrent attenuated recruitment of CD8$^+$ leukocytes in the inflamed *Dcn*$^{-/-}$ ears. The aim of this study was to elucidate the molecular pathways affected by the loss of decorin. *In vivo*, reduced numbers of CD8$^+$ cells in *Dcn*$^{-/-}$ ears correlated with a reduced interferon-γ (*Ifn-γ*) and CXCL-10 expression. *In vitro*, *Dcn*$^{-/-}$ lymphocytes displayed an increased adhesion to brain microvascular (bEnd.3) endothelial cells. Decorin treatment of bEnd.3 increased *Icam1* and down-regulated *Vcam1* expression after TNF-α stimulation. However, *Dcn*$^{-/-}$ and wild-type lymphocytes produced IFN-γ after activation with CD3ε. Upon incubation with decorin, endothelial cells and fibroblasts responded differently to IFN-γ and TNF-α; CCL2 in bEnd.3 cells was more prominently up-regulated by TNF-α compared with IFN-γ. Notably, both factors were more potent in the presence of decorin. Compared with TNF-α, IFN-γ treatment induced significantly more CXCL-10, and both factors increased synthesis of CXCL-10 in the presence of decorin. The response to IFN-γ was similar in *Dcn*$^{-/-}$ and wild-type fibroblasts, an additional source of CXCL-10. However, addition of decorin yielded significantly more CXCL-10. Notably, decorin increased the stability of IFN-γ *in vitro* and potentiated IFN-γ-induced activation of STAT-1. Furthermore, only dermatan sulfate influenced IFN-γ signaling by significantly increasing CXCL-10 expression in contrast to decorin protein core alone. Our data demonstrate that decorin modulates delayed-type hypersensitivity responses by augmenting the induction of downstream effector cytokines of IFN-γ and TNF-α, thereby influencing the recruitment of CD8$^+$ lymphocytes into the inflamed tissue.

Delayed-type hypersensitivity (DTH)[3] is a model of cell-mediated acute allergic inflammation (1). Small organic molecules are one of the important clinical categories of contact allergens that undergo haptenization. During the sensitization with the hapten oxazolone, two populations of reactive T cells are primed. CD8$^+$ cells mediate the inflammatory reaction and produce IFN-γ, 8–24 h after elicitation, to promote the killing of the haptenized cells resulting in the inflammatory reaction similar to allergic contact dermatitis (2). In chemical hapten-induced DTH, early up-regulation of TNF-α precedes IFN-γ production. TNF-α induction depends on ICAM1 expression and endothelial presentation of the hapten to CD8$^+$ cells (3). In contrast, CD4$^+$ cells limit the magnitude and duration of the reaction by producing IL-4 and IL-10 (4–6). The intensity of neutrophil infiltration controls the number of antigen-primed CD8$^+$ T cells recruited into cutaneous antigen challenge sites (7). In addition, mast cells regulate the magnitude and the cytokine microenvironment of the contact hypersensitivity response (8). Given the multitude of cell types involved in DTH, it is not surprising that this response is orchestrated by a complex network of cytokines and their receptors. For example, the DTH reaction depends on the activity of cytokines and chemokines such as TNF-α (9, 10), IL-1β (10), IL-5 (11), IL-6 (12), IL-18 (13), CXCL-9 and CXCL-10 (14), and TGFβ/Smad3 (15) or cytokine receptors such as CXCR4 (16, 17), TLR2 (18), and TLR4 (19).

* This work was supported by the Innovative Medizinische Forschung of the Medical Faculty Münster Grant I-SE 12 08 11, Deutsche Forschungsgemeinschaft Grant SE1431/3-1 (to D. G. S. and M. G.), and International Research Training Group "Molecular and Cellular GlycoSciences" Grant GRK 1549 (to A. K. U.).

[S] This article contains supplemental Figs. 1–5.

[1] Both authors contributed equally to this work and should be considered senior authors.

[2] To whom correspondence should be addressed: Institute of Physiological Chemistry and Pathobiochemistry, Waldeyerstr. 15, Münster University, UKM, 48149 Münster, Germany. Tel.: 49-251-83-55578; Fax: 49-251-83-55596; E-mail: dgseidle@uni-muenster.de.

[3] The abbreviations used are: DTH, delayed-type hypersensitivity; *Dcn*$^{-/-}$, Decorin knock-out; GAG, glycosaminoglycan; DS, dermatan sulfate; HPF, high power field; MEM, minimum Eagle's medium; PMN, polymorphonuclear neutrophil; mr, murine recombinant.

Downloaded from http://www.jbc.org/ at Istituto Superiore di Sanità on December 12, 2013

The dermatan sulfate (DS) proteoglycan decorin is involved in regulating some of these inflammatory processes. (i) It can bind to TLR2 and TLR4 followed by inducing NF-κB signaling (20). (ii) It is capable of sequestering TGF-β under fibrotic conditions (21, 22). It enhances the IFN-γ-induced expression of inducible NO synthase, TNF-α, IL-1β, and IL-6 (23). (iv) Decorin is capable of binding to TNF-α (24). (v) Decorin deficiency results in reduced IL-5 production in an experimental model of asthma (25). During inflammation monocytes are recruited from the circulation to the endothelium by the chemokine CCL2/MCP-1, which is increased in $Dcn^{-/-}$ mice (26).

It is well established that proteoglycans are capable of specifically binding to a variety of ligands relevant to allergic inflammation, either via their protein cores or the GAG side chains (27, 28). This leads to a modulation of signaling function of cytokines and chemokines and of the adhesive properties of cell adhesion molecules and integrins (27, 26). Indeed, proteoglycans and their GAGs can play a role in DTH. For example, the application of heparin or inhibition of the heparan sulfate-degrading enzyme heparanase and reduction of endothelial heparan sulfation inhibit oxazolone-mediated murine DTH (29–31). Regarding specific proteoglycans, we recently demonstrated that mice deficient in the cell surface heparan sulfate proteoglycan syndecan-1 exhibit increased integrin-dependent leukocyte recruitment and increased and prolonged edema formation during DTH, which was accompanied by increased expression of proinflammatory cytokines and ICAM1 (32). Apart from heparan sulfate proteoglycans, small leucine-rich proteoglycans can modulate various aspects of both innate and acquired inflammatory responses (33). Whereas lumican promotes neutrophil migration via binding to β2 integrins (34), biglycan promotes proinflammatory signaling via TLR2/TLR4 (35, 36). However, little is known about the involvement of these proteoglycans in DTH responses. The DS proteoglycan decorin can be detected in the plasma of patients suffering from Gram-negative or Gram-positive infections as well as healthy control persons (20, 37).

Notably, DS is required for IFN-γ presentation by mast cells to other immune cells (38), and injection of mice with DS increases the soluble levels of circulating ICAM1 (39), two processes highly relevant to the DTH response. Using an oxazolone-evoked contact allergy model in a genetic background lacking endogenous decorin, we recently reported that absence of this proteoglycan results in reduced edema formation, increased adhesion of granulocytes to endothelial cells, and concurrent reduced extravasation of leukocytes into the inflamed tissue (26). Although the early cytokine *Ccl2* was increased, the amount of TNF-α was significantly reduced in oxazolone-stimulated ears of $Dcn^{-/-}$ mice. This led us to hypothesize that decorin would affect $CD8^+$ adhesion to endothelial cells, thereby influencing the biology of adhesion molecules and cytokine expression during early allergic reactions.

In this study, we address the molecular impact of decorin and its dermatan sulfate chain on regulating the expression of IFN-γ in endothelial cells and fibroblasts and downstream effector molecules during orchestration of the acute contact allergic response *in vitro* and *in vivo*.

EXPERIMENTAL PROCEDURES

Materials and Animals—The following primary antibodies were used: rat anti-mouse Ki67 (clone TEC-3, DakoCytomation, Switzerland) and rat anti-mouse CD8α (Ly-2; Pharmingen); and donkey anti-rat immunoglobulin G (IgG; H+L)-Cy3 (Dianova). For FACS, the following were used: anti-CD4-FITC (clone YTS 191.1.2), anti-CD8α-phycoerythrin (clone YTS 169.4) (EuroBioSciences), and anti-CD183 (CXCR3)-allophycocyanin (eBiosciences). DS was generated from purified human skin fibroblast decorin (40) by β-elimination. Purification and characterization of the biologically active decorin protein core were described before (41). Samples were analyzed as described before and had no detectable levels of endotoxins (42). The following substances were used: CS4S and CS6S (Sigma), murine recombinant cytokines IFN-γ and TNF-α (R&D Systems), and mrCXCL-10 (eBiosciences). The decorin-deficient mice ($Dcn^{-/-}$) (43) and decorin/syndecan-1 double-deficient ($Dcn^{-/-}/Sdc1^{-/-}$) (26) mice were bred in the animal facility in accordance with the German Animal Protection Act and were approved by the Ethics Review Committee (8.87–50.10.36.08.299) for laboratory animals of the District Government of Münster, Germany.

Delayed-type Hypersensitivity Assay—DTH was carried out with 8–12-weeks-old male $Dcn^{-/-}$,$Dcn^{-/-}/Sdc1^{-/-}$ mice and the respective controls as described previously (26, 32). Briefly, mice were sensitized on the abdominal shaved skin with 150 μl of 2.5% oxazolone (Sigma) dissolved in acetone/ethanol (3:1 (v/v)). Mice were challenged 7 days later with 10 μl of 1% oxazolone topically administered to the ear twice. Thickness of a constant area (1 cm^2) of the ear was measured with a Mitutoyo engineer's micrometer. Decorin expression is not obviously affected in wild-type ears by oxazolone treatment (supplemental Fig. 1, *A* and *B*).

Isolation of Primary Decorin-null Fibroblasts and Lymphocytes—Skin fibroblasts were obtained from 1-day-old $Dcn^{-/-}$ mice (43) or wild-type C57BL/6 mice as described previously (44, 45). Cells were cultured in modified Eagle's minimum essential medium with Earle's salts and supplemented with 10% fetal calf serum (FCS) (Biochrom, Germany), 2 mM glutamine, and 100 units/ml penicillin, 0.1 mg/ml streptomycin (PAA, Austria). Cells were used for the subsequent experiments at passage 3. Inguinal, axillary, brachial, and cervical lymph nodes were isolated from 8-week-old male wild-type and $Dcn^{-/-}$ mice. After separation with a cell strainer (70 μm; Falcon), lymph node cells were cultured in RPMI 1640 medium (PAA, Austria) with 5% FCS, 100 units/ml penicillin, and 0.1 mg/ml streptomycin for 1 h. Nonadherent lymphocytes of supernatant were used for further experiments.

Endothelial bEnd.3 Cell Line—The bEnd.3 cell line was generated from murine brain endothelial cells (46). Cells were cultured in Dulbecco's modified Eagle's medium (PAA, Austria) supplemented with 10% FCS, 100 units/ml penicillin, and 0.1 mg/ml streptomycin in an incubator with 7.5% CO_2.

Activation of Primary Lymphocytes—Wild-type and $Dcn^{-/-}$ primary lymphocytes (2×10^6 cells/24-well) were activated by cultured the cells on anti-CD3ε-coated plates (10 μg/ml) for 6 h in complete RPMI 1640 medium (47). To increase stimula-

Downloaded from http://www.jbc.org/ at Istituto Superiore di Sanità on December 12, 2013

tion, lymphocytes were additionally treated with 10 ng/ml mrCXCL10 (48). Resting lymphocytes were cultured on non-coated plates for 6 h.

Adhesion Assays—bEnd.3 cells were used for static lymphocyte adhesion assays, as described previously (26, 49). Approximately 2×10^4 endothelial cells/well were cultured in 96-well plates overnight, followed by treatment with 85 μg/ml TNF-α to stimulate endothelial cells. After overnight stimulation, TNF-α was removed from bEnd.3 cells by washing with PBS. A total of 2.5×10^6 cells/ml lymphocytes in PBS, 1% FCS was incubated with 1 μM fluorescent marker 2′,7′-bis(2-carboxyethyl)-5-carboxyfluorescein acetoxymethyl ester (Molecular Probes, Eugene, OR) in DMSO for 20 min at 37 °C. Equal labeling efficiency was controlled using standard curves. Labeled samples were centrifuged for 5 min at 1500 rpm, and the pellet was resuspended in FCS-free medium. Thereafter, endothelial cells were incubated with resting, activated ± CXCL-10 lymphocytes (2×10^6/ml, 50 μl/well) for 15 min at 37 °C. Wells were washed two times with PBS, and adherent lymphocytes were lysed with lysis buffer (10 mM Tris/HCl, 0.1% SDS, pH 8.5). The fluorescence signal was quantified in a Spectramax fluorimeter (excitation, 485 nm; emission, 535 nm). The adhesion was reported as the number of adherent cells. The results were expressed as mean ± S.E.

Production and Purification of Human Decorin—Decorin was purified from conditioned medium of human skin fibroblasts as described before (50). The purity of decorin was verified by silver staining after SDS-gel electrophoresis. Decorin protein core purification and characterization were described previously (41).

Dermal Sheet Staining and Analysis of T Cells by FACS—A modified protocol for whole ear staining was used (51). Briefly, ears were cut off and split into two halves. The dorsal ear sites (without cartilage) were incubated in PBS, 1% FCS, 2 mM EDTA for 3–3.5 h at 37 °C. Dermal sheets were separated from the epidermis and fixed in acetone. Ear sheets were blocked in PBS, 1% FCS for 1 h at RT and immunolabeled with rat anti-mouse CD8α (625 ng/μl) overnight at 4 °C. Primary antibody was detected with donkey anti-rat immunoglobulin G-Cy3 (0.3 μg/ml). For quantification, positive cells were counted in 15–20 HPF (magnification ×40) per ear by using fluorescence microscope Imager.M1 (Zeiss, Jena) and Velocity 3D Image Analysis software (Improvision/PerkinElmer Life Sciences).

For the FACS assays, cervical lymph nodes and spleen were removed and passed through cell strainers in PBS, pH 7.4, containing 2% FCS. Blood samples were taken from heart and cleared of erythrocytes using distilled H_2O, 155 mM NH_4Cl, 10 mM $KHCO_3$ lysis buffer for 10 min on ice. Cells were washed in cold PBS, 2% FCS and stained with anti-CD4-FITC (1:200), anti-CD8α-PE (1:200), and anti-CD183 (CXCR3)-APC (1:400) for 30 min on ice. FACS analysis was performed on a FACSCalibur (BD Biosciences) and analyzed with CellQuest software (BD Biosciences). Data were compared by nonparametric analysis (GraphPad Prism software) using the Mann-Whitney *U* test for independent groups. p values <0.05 were considered as statistically significant.

Histology and Immunohistochemistry—After euthanasia of the animals, ear samples were embedded in Tissue-Tek OCT compound (Sakura Finetek, Japan). Frozen tissue blocks were cut into 5-μm sections by using a Microm HM560 (Microm International GmbH, Waldorf, Germany). Sections were fixed with methanol for 10 min at −20 °C, blocked with 1% BSA (Serva, Heidelberg, Germany)/PBS for 30 min at RT, followed by incubation with rat anti-mouse Ki67 (6.2 ng/ml) for 1 h at RT. Positive cells were detected using Cy3-labeled donkey anti-rat IgG. To rule out unspecific binding of antibodies, negative controls without primary and/or secondary antibodies were performed, respectively. Positively stained cells were counted on five slices in five high power fields (HPFs) at ×20 magnifications and expressed as cells per HPF.

Quantitative TaqMan Real Time PCR—After euthanasia of the animals, ears were excised and snap-frozen in liquid nitrogen, followed by preparation of total RNA using the RNeasy kit (Qiagen, Hilden). 1 μg of total RNA was transcribed into cDNA using Omniscript RT kit (Qiagen, Hilden, Germany) reagents according to the manufacturer's guidelines, and cDNA corresponding to 25 ng of total RNA was used as a template in PCR. Real time PCR was performed to analyze *Ifn*-γ expression in ear tissue using the 7300 real time PCR system (Applied Biosystems, Heidelberg, Germany) and TaqMan reagents (master mix and probe *Ifn*-γ (Mm00801778_m), reference gene mammalian 18 S rRNA (Hs99999901_s1) Applied Biosystems). PCR conditions were as follows: 95 °C for 10 min, followed by 40 cycles of 95 °C for 15 s and 60 °C for 1 min. Expression relative to endogenous 18 S control was determined using the $\Delta\Delta Ct$ method as described elsewhere (52). The decorin expression in bEnd.3 and wild-type fibroblasts was determined by quantitative RT-PCR using the following primers: decorin forward 5′-TGAGCTTCAACAGCATCACC-3′ and decorin reverse 5′-AAGTCATTTTGCCCAACTGC-3′; actin forward 5′-GGCTGTATTCCCCTCCATCG-3′ and actin reverse 5′-CCAGTTGGTAACAATGCCATGT-3′. For statistical analysis, Mann-Whitney *U* test was used. A $p < 0.05$ was considered statistically significant.

ELISA—The Quantikine ELISA kit (R&D Systems) was used to measure IFN-γ in protein lysates of ear tissue, as indicated by the manufacturer. For equal protein loading, a bicinchoninic acid protein assay kit (Pierce) was used to calculate protein concentration in each sample. Optimal protein concentrations were determined for IFN-γ (1.5 mg/ml). Samples were stored at −80 °C until the time of ELISA. All samples were run in triplicate. A multidetection Microplate Reader Synergy HT (Bio-Tek) was used for measurement of absorbance at 450 nm. A four-parameter curve was generated for calculation of the actual cytokine concentration. To analyze the influence of decorin on the stability of IFN-γ, FCS-free MEM was loaded with 0.5 μg/ml mrIFN-γ with/without 5 μg/ml (~100 nM) decorin. After 72 h at 37 °C, IFN-γ concentration was measured by ELISA.

Stimulation of Primary Fibroblasts—Wild-type and $Dcn^{-/-}$ primary fibroblasts were seeded at a density of 2.5×10^4 cells/96-well and cultured overnight. 24 h prior to the experiment, the 90–95% confluent cells were starved in FCS-free MEM followed by incubation for 24 h in FCS-free MEM in the presence of 0.5 μg/ml mrIFN-γ or 85 ng/μl mrTNF-α and additional treatment of 5 μg/ml decorin, decorin core, DS, CS4S, or CS6S,

Downloaded from http://www.jbc.org/ at Istituto Superiore di Sanità on December 12, 2013

TABLE 1

TaqMan low density array data of DTH-induced expression of proinflammatory genes in treated ear tissue of *Dcn*$^{-/-}$ mice

Total mRNA was isolated from treated ear tissue of two wild-type and two *Dcn*$^{-/-}$ mice 24 h after DTH induction. Values shown are the fold increase or decrease in the expression level of the indicated gene in ear tissue from *Dcn*$^{-/-}$ mice related to the expression in control/wild-type mice.

Probe no.	Gene name	Relative expression ΔCt		-Fold increase	-Fold decrease
		Wild type	*Dcn*$^{-/-}$		
Cell surface marker					
Mm00442754_m1	CD4 antigen (*Cd4*)	11.28	11.12	1.12	
Mm01182107_g1	CD8 antigen, α chain (*Cd8a*)	10.16	12.56		5.29
Interferon pathway					
Mm00801778_m1	Interferon, γ (*Ifng*)	7.46	12.98		45.74
Mm00439518_m1	Signal transducer and activator of transcription1 (*Stat1*)	4.68	6.29		3.06
Chemokines and chemokine receptor					
Mm00443258_m1	Tumor necrosis factor (*Tnfa*)	6.75	8.99		4.71
Mm00441724_m1	Transforming growth factor, β1 (*Tgfb1*)	6.57	7.27		1.62
Mm00445235_m1	Chemokine (CXC motif) ligand 10 (*Cxcl10*)	3.14	7.05		14.99
Mm00444662_m1	Chemokine (CXC motif) ligand 11 (*Cxcl11*)	5.25	9.7		21.93
Mm00439620_m1	Interleukin 1,α (*Il1a*)	7.90	8.20		1.24
Mm00434228_m1	Interleukin 1,β (*Il1b*)	4.19	5.31		2.17
Mm00445259_m1	Interleukin4 (*Il4*)	10.53	10.64		1.09
Mm00439616_m1	Interleukin 10 (*Il10*)	11.60	9.76	3.58	
Mm00439619_m1	Interleukin 17 (*Il17*)	16.34	13.91		5.35
Mm00440485_m1	Nitric-oxide synthase 2, inducible, macrophage (*Nos2*)	6.74	13.38		99.78
Mm00438259_m1	Chemokine (CXC motif) receptor 3 (*Cxcr3*)	11.19	12.91		3.29
Adhesion molecules					
Mm00441278_m1	Selectin, endothelial cell (*Sele*)	11.41	9.4	4.01	
Mm00441295_m1	Selectin, platelet (*Selp*)	11.15	10.66	1.41	
Mm00449197_m1	Vascular cell adhesion molecule1 (*Vcam1*)	9.30	10.31		2.00

respectively. Cell culture supernatants were stored at −20 °C until analysis of CXCL-10 by ELISA.

CXCL-10 Expression of Primary Fibroblasts—CXCL-10 was detected in supernatant of stimulated fibroblasts by an ELISA according to the manufacturer's instructions (RayBiotech). 30 μl of fibroblast supernatant were used for CXCL-10 measurement. All samples were run in triplicate. Data were analyzed by a two-tailed paired *t* test (GraphPad Prism software). $p < 0.05$ was considered as statistically significant.

Stimulation of Endothelial bEnd.3 Cell Line—Approximately 2×10^5 bEnd.3 cells/24-well plate were cultured in FCS-free DMEM for 24 h and stimulated 0.5 μg/ml mrIFN-γ or 85 ng/ml mrTNF-α ± decorin. DMEM was supplemented with penicillin and streptomycin. Cell culture supernatants were stored at −20 °C until analysis of CXCL-10 and CCL2 by ELISA. Because bEnd.3 cells expressed decorin mRNA under our culture conditions, we performed decorin siRNA knockdown followed by CXCL-10 ELISA. For siRNA transfection, bEnd.3 cells were plated in a 24-well plate 1 day prior to transfection to reach 80% confluency after 24 h. Transfection was performed using Dharmafect reagent (Dharmacon Lafayette, CO) in Opti-MEM medium (Invitrogen) and Silencer Select siRNA s64858, targeting the coding region of *Dcn* (20 nM) and negative control siRNA 1 (20 nM) (Applied Biosystems, Darmstadt, Germany) according to the manufacturer's instructions. 24 h after transfection, Opti-MEM was replaced by DMEM. CXCL-10 ELISA was performed 24 h after transfection as indicated under "Results."

CXCL-10 and Ccl2 Expression of Stimulated bEnd.3 Cell Line—CXCL-10 was detected by ELISA in the supernatant of stimulated bEnd.3 cells (RayBiotech), according to the manufacturer's instructions. 20 μl of bEnd.3 cell supernatant were used for to CXCL-10 measurement. CCL2 expression of bEnd.3 cells was determined by the Quantikine ELISA kits (R&D Systems). Cell supernatant was diluted 1:150. All samples were run in triplicate. Data were analyzed by a two-tailed paired *t* test (GraphPad Prism software). $p < 0.05$ was considered as statistically significant.

Peroxidase Activity Assay—As a measure of total granulocyte infiltration, we determined peroxidase activity of protein samples as described previously (53). Briefly, 3,3′,5,5′-tetramethylbenzidine (Sigma) was used as a sensitive chromogen substrate for peroxidase. 24 h after DTH induction ears of wild-type, *Dcn*$^{-/-}$, *Sdc1*$^{-/-}$, and *Dcn*$^{-/-}$/*Sdc1*$^{-/-}$ mice were taken and lysed. 15 μg of protein lysates and 100 μl of 3,3′,5,5′-tetramethylbenzidine solution were added to a microtiter plate to start the reaction. After 20 min of incubation at room temperature, the reaction was stopped with 50 μl of 2 M H_2SO_4. Absorbance was measured at 450 nm.

RESULTS

Recently, we could show that the loss of decorin leads to a reduced allergic reaction during DTH (26). To elucidate the underlying mechanism, we analyzed the cytokine expression profile *in vivo* and confirmed these results *in vitro* using endothelial cells and fibroblasts, which are involved in the DTH.

Differential Expression of Proinflammatory Cytokines Evoked by Decorin—TaqMan low density array analysis (mouse immune panel from Applied Biosystems) of ear tissue of wild-type and *Dcn*$^{-/-}$ mice subjected to oxazolone-mediated DTH reactions showed that several cytokines out of 96 genes were differentially regulated at the mRNA level by the loss of decorin during DTH (Table 1). 6.7% of the genes were up-regulated; 23.2% were down-regulated, and 64.4% were not altered. Looking at effector cell markers of DTH, *Cd8a* was markedly down-regulated in the decorin-deficient background in contrast to *Cd4*, which was not altered. Additional genes negatively affected by the lack of decorin included IFN-γ, synthesized by

Downloaded from http://www.jbc.org/ at Istituto Superiore di Sanità on December 12, 2013

$CD8^+$ cells and NO synthase (Table 1). $CD8^+$ cells are an important component in the response to hapten-mediated allergic reactions (3). To independently confirm the expression results obtained by the array, we analyzed $CD8^+$ cells on a cellular level.

$CD8^+$ Cells Are Reduced in $Dcn^{-/-}$ Ears during DTH—The down-regulation of *Cd8* mRNA is in line with our previous results of a reduced $CD8^+$ immunostaining in the inflamed ears of $Dcn^{-/-}$ mice. However, this difference was not significant (26). This could be related to a significant increase in $CD8^+$ cells in the blood of naive $Dcn^{-/-}$ mice (Fig. 1, *A* and *B*; $n = 9$). Twenty four h after oxazolone treatment, $Dcn^{-/-}$ blood showed also more $CD8^+$ cells (not significant) (Fig. 1*B*), whereas after 48 h the difference in $CD8^+$ cells was again significantly higher in $Dcn^{-/-}$ mice compared with wild-type (Fig. 1*B*; $n = 9$; $p \leq 0.01$). Therefore, we analyzed the oxazolone-treated ears again using improved methodology. Dermal sheet staining allowed for a more sensitive detection of $CD8^+$ cells compared with staining of cryosections. Interestingly, $CD8^+$ leukocytes were significantly reduced in $Dcn^{-/-}$-inflamed ears compared with wild-type (Fig. 1, *C* and *D*; $n = 6$; $p \leq 0.01$). To exclude the possibility that this reduction was due to changes in proliferation, we immunostained for the proliferation marker Ki67, and we found no differences between the two genotypes (supplemental Fig. 2).

IFN-γ Expression Is Affected by the Loss of Decorin during DTH at Early Time Points—First, we evaluated the results obtained for *Ifn-γ* by the immune panel array that showed an ~46-fold reduction of this cytokine in the decorin-null background tissue (Table 1). Next, we validated these changes by quantitative PCR and confirmed that the *Ifn-γ* mRNA expression was significantly reduced in $Dcn^{-/-}$ mice (Fig. 2*A*). Furthermore, this could be confirmed by a significant and substantial reduction of IFN-γ protein in $Dcn^{-/-}$ ear tissue (Fig. 2*B*). We note that this is a dynamic process insofar as at 48 h both mRNA and protein levels of IFN-γ returned to basal levels (Fig. 2, *A* and *B*).

As $CD8^+$ cells produce IFN-γ, we tested whether lymphocytes of $Dcn^{-/-}$ mice were able to synthesize IFN-γ, one of the key cytokines mediating DTH (54). For this purpose, $Dcn^{-/-}$ and wild-type lymphocytes were stimulated for 24 h with either concanavalin A or decorin followed by an IFN-γ ELISA. As expected, exogenous decorin did not induce IFN-γ in both strains of lymphocytes (Fig. 2*C*, $n = 3$). In contrast, the lectin concanavalin A triggered *Ifn-γ* expression in wild-type and $Dcn^{-/-}$ cells to the same extent. No obvious difference in lymph node morphology was observed between 8-week-old wild-type and $Dcn^{-/-}$ mice (supplemental Fig. 1*C*).

To detect lymphocyte activation, we next used a CD3ε antibody that reacts with the 25-kDa chain of the T cell receptor-associated CD3 complex (47). We found that *Ifn-γ* expression increased in both $Dcn^{-/-}$ and in wild-type cells (Fig. 2*D*, $n = 3$, $p = 0.4$), indicating that $Dcn^{-/-}$ lymphocytes are able to express IFN-γ. Apart from IFN-γ, expression of the Th2 cytokine IL-10 was changed according to the TaqMan array data. However, at the protein level, there were no significant changes between oxazolone-stimulated $Dcn^{-/-}$ and wild-type mouse ears (data not shown).

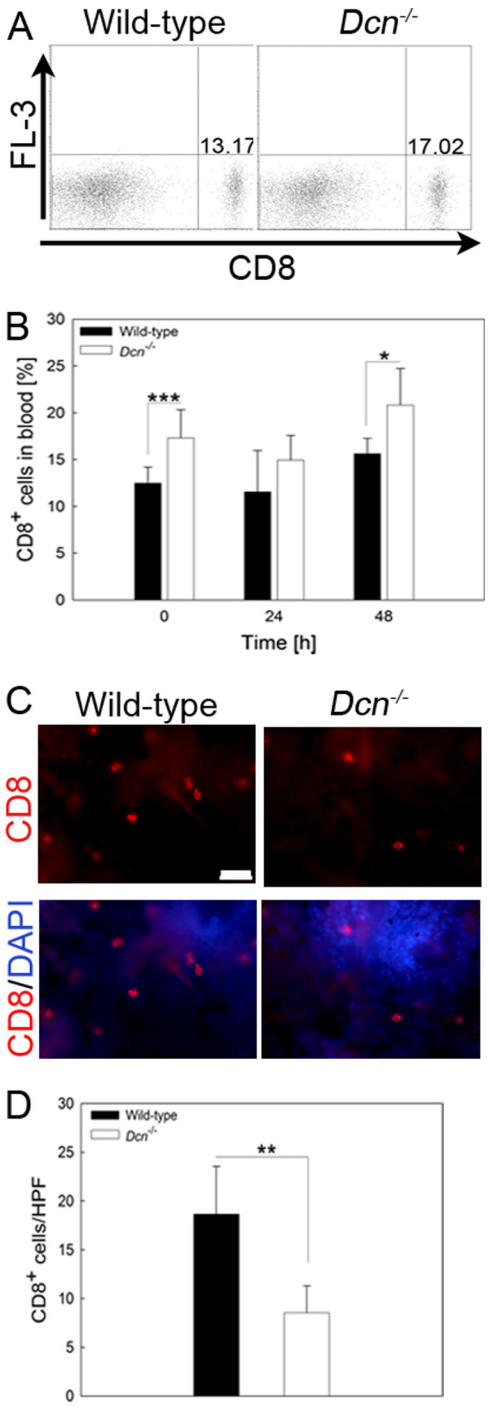

FIGURE 1. **Distribution of $CD8^+$ cells in blood and ear tissue of $Dcn^{-/-}$ and wild-type mice during DTH.** *A*, *upper panel* displays a representative FACS staining for $CD8^+$ cells in blood of naive wild-type and $Dcn^{-/-}$ (numbers in %). *B*, quantification shows a significant increase of $CD8^+$ cells in blood of naive $Dcn^{-/-}$ mice even after 48 h of DTH induction ($n \geq 6$; ***, $p < 0.005$; *, $p < 0.05$; mean ± S.D.). *C*, to analyze $CD8^+$ cell infiltration into inflamed tissue, whole ears of wild-type and $Dcn^{-/-}$ mice were fluorescence-stained for CD8; *bar*, 25 μm. *D*, quantification shows that the total amount of $CD8^+$ cells is reduced in $Dcn^{-/-}$ mice compared with wild type 24 h after DTH induction ($n = 6$; **, $p < 0.01$; mean ± S.D.).

Endothelial Adhesion of $Dcn^{-/-}$ Lymphocytes is Increased under Basal, but Not under CD3ε/CXCL-10-induced Conditions—As we showed previously that $Dcn^{-/-}$ neutrophils and polymorphonuclear cells display an increased adhesion to

Downloaded from http://www.jbc.org/ at Istituto Superiore di Sanità on December 12, 2013

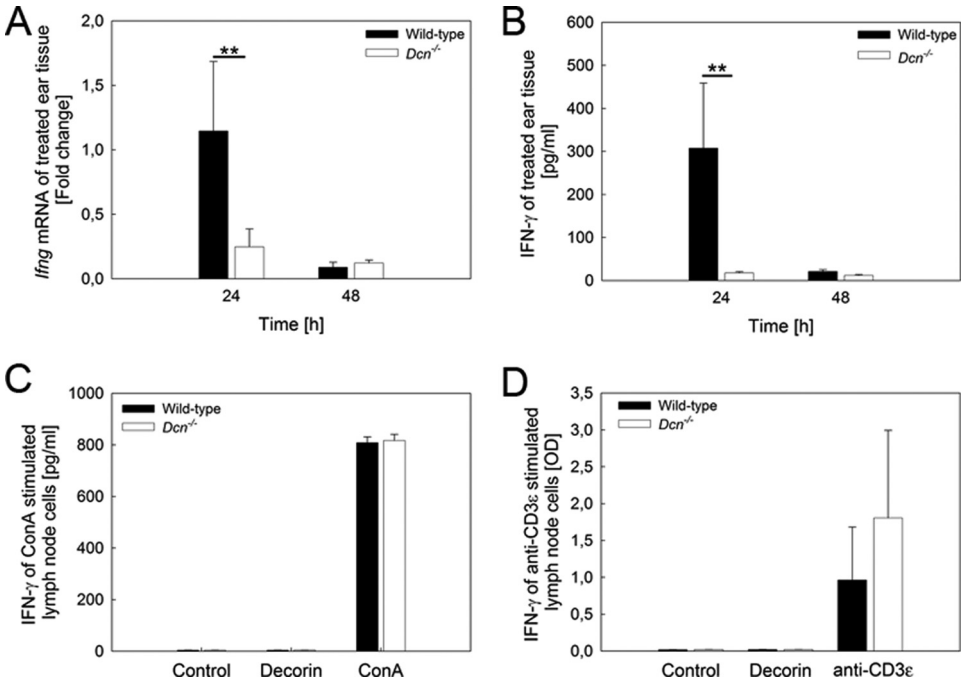

FIGURE 2. **IFN-γ expression is affected by the loss of decorin during DTH at early time points.** At the mRNA level, $Dcn^{-/-}$ mice show significantly decreased *Ifn*-γ expression in ear tissue 24 h after DTH induction (*A*, $n = 4$, **, $p < 0.01$). This also results in a reduced amount of IFN-γ protein (*B*, $n = 4$, **, $p < 0.01$). To test whether $Dcn^{-/-}$ lymphocytes are capable of synthesizing IFN-γ to the same extent as the wild type, we cultured lymph node cells in the presence of concanavalin A (*C*) and on anti-CD3ε-coated plates (*D*). The subsequent measurement of IFN-γ shows no difference between the two strains. *C* shows one example out of three independent experiments, and *D* is the summary of three independent experiments. Values shown are in mean ± S.D. ($n = 3$, $p = 0.4$).

endothelial cells, we next analyzed adhesiveness of lymphocytes. We first examined the influence of activation by CD3ε on adhesion of lymphocytes to TNF-α stimulated bEnd.3 endothelial cells. We found a significantly increased adhesion of resting $Dcn^{-/-}$ lymphocytes to TNF-α-stimulated endothelial cells as compared with wild type (Fig. 3*A*). Interestingly, CD3ε activation of lymphocytes differentially affected adhesion of $Dcn^{-/-}$ cells as compared with wild-type cells. Lymphocyte activation resulted in an increased adhesion of wild-type cells but not for $Dcn^{-/-}$ cells. Using the chemokine CXCL-10 as a co-stimulant, wild-type but not $Dcn^{-/-}$ lymphocyte adhesion significantly increased further. Notably, we obtained a significant decrease compared with $Dcn^{-/-}$ resting lymphocytes (Fig. 3*A*; $n = 5$, *, $p < 0.05$; ***, $p < 0.001$), indicating that under static conditions $Dcn^{-/-}$ lymphocytes behave differently than the wild-type cells.

Cytokine Receptor Expression Is Not Altered in $Dcn^{-/-}$ Mice—These results presented above raise the possibility that the expression of cytokine receptors could be affected by the genetic ablation of *Dcn*. To address this point, we analyzed the expression of CXCR3, the receptor for CXCL-10, CXCL-9, and CXCL-11, as its mRNA was reduced by ~3-fold in the array (Table 1). FACS analysis of circulating leukocytes revealed that the amount of double-positive $CD4^+/CXCR3^+$ and $CD8^+/CXCR3^+$ leukocytes was not significantly altered in $Dcn^{-/-}$ mice under neither naive nor inflammatory conditions (Fig. 3, *B–E*, $n = 3$). Furthermore, the expression of *Ifn*-γ receptor 1 and 2 in ear tissue showed no differences between the two strains under neither inflammatory nor control conditions (data not shown). $Dcn^{-/-}$ mice showed several alterations in the cytokine profile according to the TaqMan low density array, which could only partially be confirmed at the protein level. For the expression for CXCL-10 protein, the downstream cytokine induced by IFN-γ, we could confirm a significant reduction by the loss of decorin (Fig. 3*F*, $n = 6$; *, $p < 0.05$).

Sdc1 Deficiency Rescues the $Cd8^+$ Phenotype of $Dcn^{-/-}$ Mice—The results above suggested that decorin could affect adhesion and/or cytokine expression during hapten-induced contact allergy. We have previously demonstrated that loss of *Sdc1* in a $Dcn^{-/-}$ background rescues the DTH phenotype (26). Therefore, we analyzed the distribution of the $CD8^+$ cells in the $Dcn^{-/-}/Sdc1^{-/-}$ mice. We discovered that the number of $CD8^+$ cells was increased by ~3-fold in the double knock-out mice as compared with $Dcn^{-/-}$ mice (Table 2), indicating that the loss of *Sdc1* rescues the $CD8^+$ phenotype of the $Dcn^{-/-}$ mice. Interestingly, the $Dcn^{-/-}/Sdc1^{-/-}$ mice had the same amount of Ifn-γ as the $Dcn^{-/-}$ mice but significantly less compared with wild-type mice (Table 2). Collectively, these results suggest that the loss of *Sdc1* cannot compensate for the effects of decorin on IFN-γ. However, the inflammatory response to oxazolone can be explained by a significant compensatory increase in neutrophils detected by peroxidase activity in the $Dcn^{-/-}/Sdc1^{-/-}$ mice (Table 2), but not in the $Dcn^{-/-}$ mice (Fig. 3*G*, $n = 3$; **, $p < 0.01$).

Decorin Modulates Production of the Cytokines CXCL-10 and CCL2 in b.End3 Endothelial Cells—As the array analysis was based on whole ear tissue composed of several cell types, we decided to determine cell type-specific effects of decorin in a less complex *in vitro* system using an endothelial cell line and primary fibroblasts. Because of high variability of CXCL-10 expression within the ear tissue, and the altered adhesion of the leukocytes, we analyzed the impact of decorin on adhesion mol-

Downloaded from http://www.jbc.org/ at Istituto Superiore di Sanità on December 12, 2013

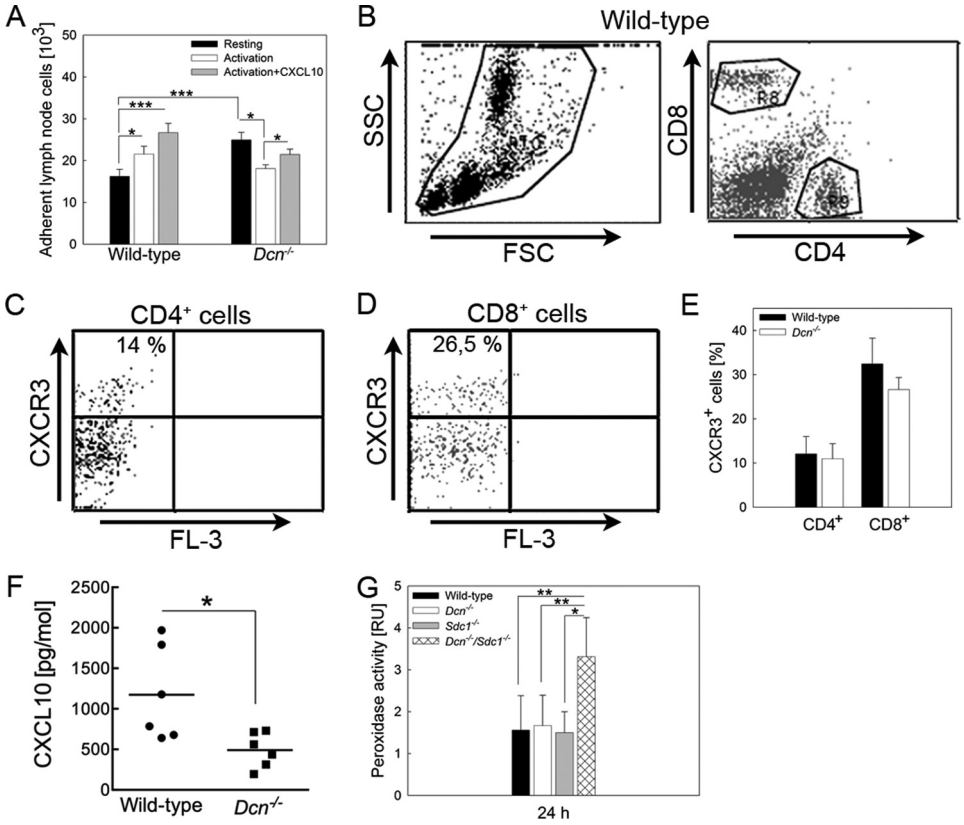

FIGURE 3. **Loss of decorin affects lymphocyte adhesion.** Lymphocytes of wild-type and $Dcn^{-/-}$ mice were isolated, partly activated by anti-CD3ϵ, and stimulated with CXCL-10. Adhesion of resting $Dcn^{-/-}$ lymphocytes was significantly increased compared with the wild-type analyzed by static adhesion experiments (*black bars*) (*A*, mean ± S.E.). This was not observed with activated lymphocytes (*white* and *gray bars*). After activation and activation + CXCL-10 stimulation, wild-type lymphocytes are increasing their adhesion to bEnd.3 cells. Interestingly, activated $Dcn^{-/-}$ lymphocytes show a significantly decreased adhesion. *B–E*, blood cells from wild-type and $Dcn^{-/-}$ mice (24 h) were co-stained for CD4, CD8, and CXCR3. *B–D* show the FACS strategy used to analyze CXCR3 expression of T cells in blood. First, blood cells were gated by their size (forward scatter, *FSC*) and their granularity (side scatter, *SSC*) (*B*). Subsequently, $CD4^+$ (*C*) and $CD8^+$ (*D*) cells were gated, and these populations were analyzed for the percentage of $CXCR3^+$ cells. Quantification of $CD4^+$ and $CD8^+$ cells (*E*) exhibits no difference between $CXCR3^+$ T cells from wild-type and $Dcn^{-/-}$ blood 24 h after DTH induction (mean ± S.D., $p_{CD4} = 0.662$ and $p_{CD8} = 0.082$). Calculated to all blood leukocytes, 2–3% were found to be double-positive for $CD4^+/CXCR3^+$ or $CD8^+/CXCR3^+$. *F*, CXCL-10 expression (mean ± S.D.) in treated ear tissue of wild-type and $Dcn^{-/-}$ mice was analyzed by ELISA where a significant reduction was determined. ($n = 6$, *, $p < 0.05$). Peroxidase activity was measured in protein lysates as marker for neutrophil infiltration into the ears (*G*, mean ± S.D.). An increased infiltration of neutrophils was detected in ears of the $Dcn^{-/-}/Sdc1^{-/-}$ mice compared with wild-type, $Dcn^{-/-}$, and $Sdc1^{-/-}$ mice ($n \geq 3$, *, $p < 0.05$; **, $p < 0.005$; ***, $p < 0.001$).

TABLE 2

Leukocyte infiltration and expression of proinflammatory cytokine IFN-γ and TNF-α in oxazolone-treated ear tissue 24 h after DTH induction

Infiltration of $CD4^+$ cells and macrophages was analyzed on cross-section of inflamed ear tissue. $CD8^+$ cells were detected by whole mount staining of the dermis form-treated ears. Peroxidase activity as marker for the neutrophil infiltration was measured in protein lysates of ear tissue. Peroxidase activity in treated ears was related to untreated wild-type samples (mean ± S.D., $n \geq 3$). AU means arbitrary units.

	Wild type	$Dcn^{-/-}$	*p* value	$Dcn^{-/-}/Sdc1^{-/-}$	*p* value
$CD4^+$ cell infiltration (cell/HRP)	11.49 ± 2.28[a]	10.80 ± 2.98[a]	0.758	10.92 ± 3.27	0.687
$CD8^+$ cell infiltration (cell/HRP)	18.64 ± 2.2	8.53 ± 1.13	[b]	21.69 ± 2.74	0.730
Peroxidase activity (AU)	1.56 ± 0.23	1.67 ± 0.19	0.612	3.31 ± 0.35	[b]
TNF-α (pg/ml)	39.0 ± 11.9[a]	18.1 ± 4.0[a]	[c]	17.7 ± 5.8	[c]
IFN-γ (pg/ml)	307.4 ± 338.9	17.5 ± 6.6	[b]	19.9 ± 5.5	[c]

[a] Data are from Ref. 26.
[b] $p < 0.005$. The *p* values compare wild type and the respective knock-out.
[c] $p < 0.05$.

ecules and chemokine expression in stimulated endothelial cells *in vitro*. Interestingly, decorin treatment significantly increased *Icam1* expression in bEnd.3 cells but had no additive effect because TNF-α treatment alone showed the same 5-fold increase as combined decorin and TNF-α treatment (Fig. 4*A*; $n = 3$; **, $p < 0.01$). Furthermore, *Vcam1* expression was also significantly increased by decorin or TNF-α treatment (Fig. 4*B*, $n = 3$; **, $p < 0.01$). Surprisingly, decorin + TNF-α led to a significant reduction in *Vcam1* mRNA compared with TNF-α alone, indicating that decorin negatively regulated the expression of adhesive proteins (Fig. 4*B*; $n = 3$).

To determine whether endothelial cells produce more CCL2 in the presence of exogenous decorin, bEnd.3 cells were either treated with TNF-α or IFN-γ and in the presence of 5 μg/ml (~100 nM) decorin. TNF-α-induced CCL2 synthesis was significantly increased compared with IFN-γ (Fig. 4*C*). TNF-α-induced CCL2 synthesis was significantly inhibited by decorin or the decorin protein core (Fig. 4*E*). To exclude that endogenous

Downloaded from http://www.jbc.org/ at Istituto Superiore di Sanità on December 12, 2013

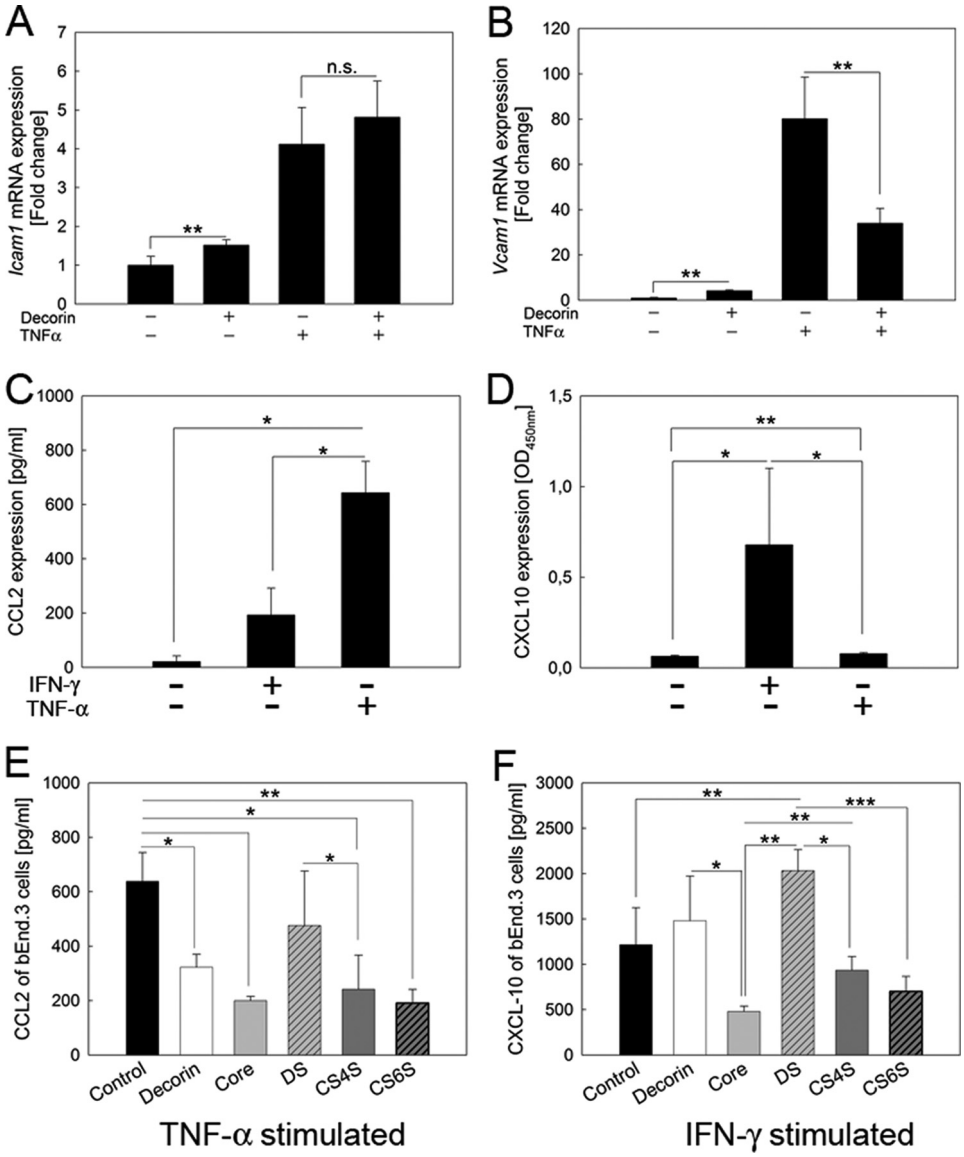

FIGURE 4. **Expression of adhesion molecules and cytokines is differentially altered by decorin in the bEnd.3 endothelial cell line.** *Icam1* mRNA expression is induced by decorin and TNF-α. Decorin and TNF-α together show no additive effects (*A*). *Vcam1* mRNA expression is also induced by decorin or TNF-α alone. Interestingly, *Vcam1* expression is inhibited by decorin + TNF-α co-treatment (*B*). *C* and *D*, bEnd.3 cells were stimulated with either IFN-γ or TNF-α for 24 h after 24 h of starvation. Cells were harvested and analyzed by an ELISA for CCL2 (*C*) or CXCL-10 (*D*). *C*, basal expression of CCL2 was very low. Both IFN-γ and TNF-α significantly induced the CCL2 production; however, TNF-α to a higher extent compared with IFN-γ. *D*, CXCL-10 expression was significantly increased by IFN-γ as well as TNF-α; however, the effect was much more prominent by IFN-γ. Data are the mean ± S.D. ($n = 5$; *, $p < 0.05$; **, $p < 0.01$). *E* shows TNF-α-stimulated bEnd.3 cells co-cultured with 5 μg/ml (protein concentration) decorin, core protein, or GAGs; subsequently, CCL2 was measured. CCL2 was significantly decreased by treatment with decorin, core protein, CS4S, or CS6S compared with cells only stimulated with TNF-α. CCL2 reduction of DS cultured cells was not significant. *F* shows CXCL-10 expression of IFN-γ stimulated bEnd.3 cells co-cultured with decorin, core protein, or GAGs. Core protein, CS4S-, or CS6S-treated cells show no significant decrease in CXCL-10 expression compared with cells only stimulated with IFN-γ, whereas CXCL-10 production was slightly increased by decorin and significantly by DS treatment compared with IFN-γ-stimulated bEnd.3 cells ($n \geq 3$, *, $p < 0.05$; **, $p < 0.01$; ***, $p < 0.005$, mean ± S.D.). *n.s.*, not significant.

decorin expressed by bEnd.3 cells is influencing the results, we determined that decorin synthesis was not influenced by either TNF-α or IFN-γ (supplemental Fig. 3*A*). In contrast to DS from skin fibroblast decorin, CS6S and CS4S significantly inhibited TNF-α-induced CCL2 synthesis (Fig. 4*E*). It is well established that one of the key downstream factors induced by IFN-γ is CXCL-10 (54). In agreement with these findings, we found that bEnd.3 cells produced CXCL-10 after IFN-γ treatment (Fig. 4*D*). The impact of TNF-α on the synthesis of CXCL-10 is smaller compared with IFN-γ (Fig. 4*D*). In contrast, treatment with decorin alone only slightly increased CXCL-10 above basal levels. Furthermore, IFN-γ + decorin but not IFN-γ + decorin protein core treatment showed the same effect on CXCL-10 synthesis as IFN-γ alone (Fig. 4*F*); however, DS derived from skin fibroblast decorin and IFN-γ significantly induced CXCL-10 levels compared with IFN-γ. CS6S and CS4S did not show an effect (Fig. 4*F*). CXCL-10 expression was not influenced by the presence of endogenous decorin, because we determined a similar expression in bEnd.3 upon siRNA knockdown of decorin (supplemental Fig. 3, *B* and *C*).

Next, as we observed an increased adhesion in $Dcn^{-/-}$ cells, we analyzed the impact of TNF-α and decorin on adhesion

Downloaded from http://www.jbc.org/ at Istituto Superiore di Sanità on December 12, 2013

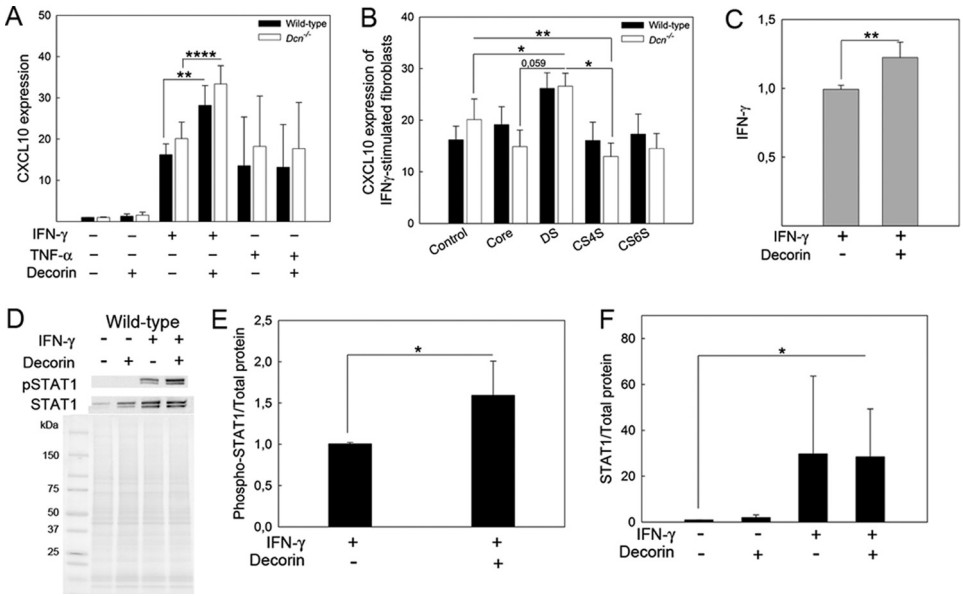

FIGURE 5. **Fibroblasts produce more CXCL-10 in the presence of decorin or DS.** Wild-type and $Dcn^{-/-}$ fibroblasts were cultured for 24 h under serum-free conditions in the presence of TNF-α or IFN-γ (*A*). TNF-α is inducing CXCL-10 in fibroblasts but to a lesser extent compared with IFN-γ. Furthermore, both cell types, wild-type and $Dcn^{-/-}$, express similar amounts of CXCL-10 after treatment with either TNF-α or IFN-γ. However, only IFN-γ stimulation is increased if 5 μg/ml (protein concentration) decorin is present. To evaluate which part of decorin is responsible for the increased CXCL-10 expression, fibroblasts were treated with IFN-γ and different GAGs (5 μg/ml). *B* shows that only DS is increasing the amount of CXCL-10 in IFN-γ-stimulated fibroblasts. In contrast, neither CS4S, CS6S, nor the core protein increased CXCL-10 expression. CXCL-10 data are the mean ± S.D. ($n = 5$; *, $p < 0.05$; **, $p < 0.01$; ***, $p < 0.005$). *C*, IFN-γ-containing conditioned medium was incubated with/without decorin for 72 h followed by an ELISA for IFN-γ. The proteoglycan decorin significantly increases the stability of IFN-γ. *D*, wild-type fibroblasts treated for 24 h with IFN-γ were analyzed by Western blot for the transcription factor STAT-1 and pSTAT-1. STAT-1 is induced by IFN-γ but not by decorin. However, IFN-γ + decorin treatment leads to a significant pSTAT-1 increase compared with IFN-γ alone. *E* and *F*, Densitometric quantitation of Western blots for pSTAT1 (*E*) and STAT-1 (*F*). Data are the mean ± S.D. ($n = 3$; *, $p < 0.05$).

molecule expression by endothelial cells. To exclude changes in the *Ifn*-γ receptor expression, mRNA was analyzed in stimulated and unstimulated bEnd.3 cells. There was no difference in the expression of the two *Ifngr1* and *Ifngr2* in bEnd.3 cells treated with decorin, IFN-γ, or IFN-γ + decorin and the respective controls (data not shown).

Fibroblasts Produce More CXCL-10 in the Presence of Decorin or Dermatan Sulfate—To demonstrate that fibroblasts can produce the downstream cytokine CXCL-10 after stimulation with either TNF-α or IFN-γ, cells were cultured for 24 h in the presence of the two cytokines, and CXCL-10 was detected by ELISA (Fig. 5*A*). IFN-γ and, to a lesser extent, TNF-α induced CXCL-10 synthesis in cultured fibroblasts. To determine the influence of endogenous decorin in wild-type fibroblasts, quantitative RT-PCR was performed. There is a basal decorin expression that is up-regulated by TNF-α but not by IFN-γ treatment (supplemental Fig. 3*A*). Furthermore, fibroblasts derived from wild-type and $Dcn^{-/-}$ mice expressed similar amounts of CXCL-10 after treatment with either TNF-α or IFN-γ. However, only the effect of IFN-γ stimulation on CXCL-10 up-regulation was significantly enhanced by decorin, whereas the stimulatory effect of TNF-α was not influenced by this proteoglycan (Fig. 5*A*). The expression for the *Ifngr1* and *-2* showed no changes between wild-type and $Dcn^{-/-}$ fibroblasts (data not shown). To evaluate which constituent (protein core *versus* GAG) of decorin was responsible for this stimulatory effect, we tested fibroblasts for their biochemical response to combined treatments with IFN-γ and different GAGs, purified from skin fibroblast decorin (DS) or obtained from Sigma (CS6S, CS4S). We discovered that only the combination of IFN-γ + DS significantly enhanced the expression of CXCL-10 in $Dcn^{-/-}$ but not in wild-type fibroblasts (Fig. 5*B*). In contrast, decorin protein core, CS6S and CS4S, had no effect. To test whether the DS proteoglycan decorin would influence the stability of IFN-γ, FCS-free MEM containing IFN-γ was analyzed. The medium was supplemented with/without decorin and incubated for 72 h. IFN-γ ELISA showed that the proteoglycan decorin increased the stability of IFN-γ (Fig. 5*C*). To demonstrate that decorin-evoked stabilization of IFN-γ would affect the cytokine signaling pathway, we determined the status of the transcription factor STAT-1 in fibroblasts exposed to the conditioned medium. Although IFN-γ treatment resulted in a significant increase in total STAT-1 levels compared with the untreated fibroblasts, decorin treatment had no impact. Analysis of STAT-1 activation, however, showed that combined decorin + IFN-γ treatment significantly increased STAT-1 phosphorylation as compared with IFN-γ alone (Fig. 5*D*). Notably, the levels and phosphorylation status of STAT-3, a transcription factor that can form heterodimers with STAT-1, were not influenced by decorin (supplemental Fig. 4). Moreover, no significant influence of decorin on NF-κB activation was observed in our experimental system (supplemental Fig. 5).

DISCUSSION

We have previously demonstrated that loss of decorin leads to a reduced DTH response *in vivo* (26), suggesting a novel and important role for this proteoglycan in modulating allergic inflammation. In this study, we have identified multiple mechanistic components of the allergic response that are modulated by decorin. Our current working model is depicted in Fig. 6.

Downloaded from http://www.jbc.org/ at Istituto Superiore di Sanità on December 12, 2013

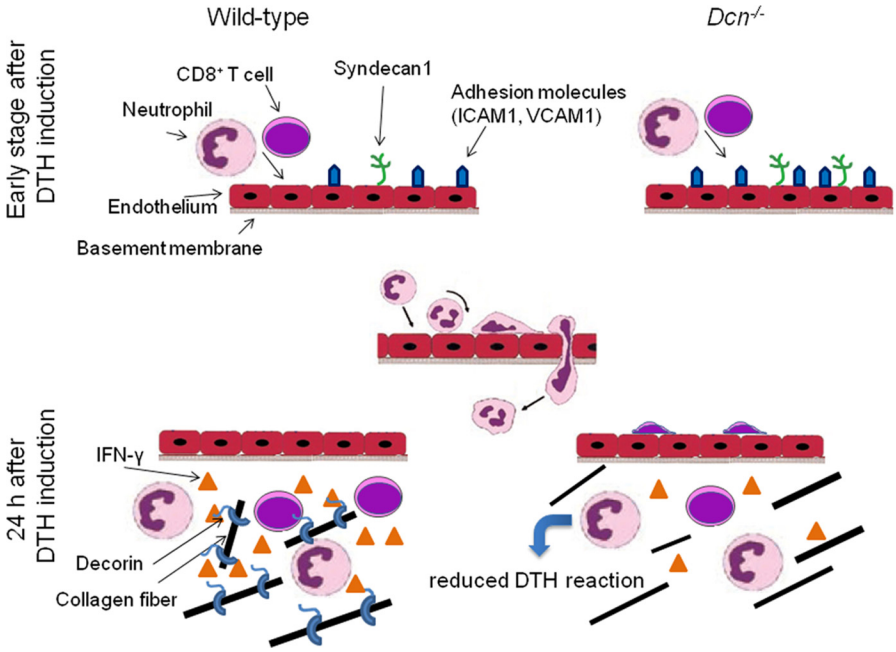

FIGURE 6. **Working model depicting the potential role of soluble decorin during phases of acute inflammation.** The *middle panel* shows the sequential steps of leukocyte recruitment and diapedesis during inflammation (27). For additional details refer to the text.

Accordingly, within the 1st h after DTH induction the expression of adhesion molecules and leukocyte-recruiting chemokines is increased (phase 1). At this stage, no appreciable alteration of leukocyte recruitment is observed between wild-type and $Dcn^{-/-}$ mice; however, $Dcn^{-/-}$ mice show an increased expression of adhesion molecules and SDC1. In the following stage, ~24 h after DTH induction (phase II), $CD8^+$ T cells, the main source of the proinflammatory cytokine IFN-γ during hapten-induced DTH reaction, enter the inflamed tissue. Notably, in $Dcn^{-/-}$ mice there is a specific low number of $CD8^+$ cells in contrast to the detectable number of other immune cells such as $CD4^+$ cells, macrophages, and neutrophils. The reduced numbers of $CD8^+$ cells in $Dcn^{-/-}$ mice contribute to a further attenuation of IFN-γ levels. Additionally, the IFN-γ seems to be less stable in the tissue of $Dcn^{-/-}$ mice. Thus, we conclude that a combination of decreased infiltration of $CD8^+$ cells and IFN-γ expression can mechanistically explain the reduced DTH response in $Dcn^{-/-}$ mice.

Notably, $CD8^+$ cells were only partially able to extravasate into the skin after oxazolone treatment. These $CD8^+$ cells mediate the DTH reaction by producing IFN-γ (3) that is barely detectable in oxazolone-treated $Dcn^{-/-}$ mouse ears, indicating that the loss of decorin not only inhibits the extravasation but also the synthesis of IFN-γ. These findings may represent a secondary consequence of altered lymphocyte recruitment, as $CD8^+$ cells are the major source of IFN-γ production during allergic reactions (3, 4), and because $Dcn^{-/-}$ lymphocytes can synthesize this cytokine upon *in vitro* stimulation. In accordance with our findings regarding $CD8^+$ cells, adhesion of $Dcn^{-/-}$ PMNs to endothelial cells is increased *in vivo* and *in vitro* (26). Moreover, peritoneum-derived PMNs deficient in the decorin-related proteoglycan lumican show differential adhesion compared with bone marrow PMNs (37). In contrast to these cell types, $CD8^+$ cells are not affected in $Dcn^{-/-}$ mice (26). Trans-endothelial $CD4^+$ and $CD8^+$ recruitment relies on different mechanisms and depends on the presence of recycling receptors such as CLEVER-1 (55) and hepatocyte growth factor, a cytokine modulated by decorin (56, 57). *In vitro*, $Dcn^{-/-}$ lymphocyte adhesion to bEnd.3 endothelial cells is also increased relative to wild type. As a potential modulator of inflammation, decorin can affect the expression of proteins in endothelial cells (58). Decorin treatment increased *Icam1* expression in bEnd.3 cells and differentially up-regulated *Vcam1* expression. Under TNF-α-stimulated conditions, decorin treatment reduced *Vcam1* expression, which could explain the increased adhesion of $Dcn^{-/-}$ cells like PMNs or even fibroblasts (26, 59). Although a potentially altered microvascular development in the absence of decorin may influence $CD8^+$ extravasation, we did not observe obvious changes in the diameter of the blood vessels (26). Bone marrow transplants demonstrated that $Dcn^{-/-}$ leukocytes in a wild-type environment also show an increased adhesion and a reduced transmigration (26) indicating that a wild-type endothelium is not sufficient to support the transmigration.

We have previously discovered that decorin loss affects *Sdc1* expression and that the $Dcn^{-/-}/Sdc1^{-/-}$ mice behave like the wild type in the hapten-induced contact allergy model (26). This is not due to the $CD8^+$ cells, as the loss of *Sdc1* can compensate for the transmigration defect of the $Dcn^{-/-}$ cells in $Dcn^{-/-}/Sdc1^{-/-}$ mice. Indeed, $Sdc1^{-/-}$ mice show the same edema formation as wild type, 24 h after DTH induction (32). Mechanistically, the $Dcn^{-/-}/Sdc1^{-/-}$ mice show the same amount of Icam1 compared with wild-type mice (26). The inflammatory response in the $Dcn^{-/-}/Sdc1^{-/-}$ mice appears to be similar to the wild-type response due to a compensatory increase in infiltrating neutrophils. Along these lines, PMNs derived from this mouse show increased adhesion to blood vessels during intravital microscopy (26). Whereas the decorin-de-

Downloaded from http://www.jbc.org/ at Istituto Superiore di Sanità on December 12, 2013

pendent CD8$^+$ transmigration phenotype could be compensated by deletion of *Sdc1*, decorin is still required for maintaining IFN-γ function. The finding of low levels of IFN-γ in *Dcn*$^{-/-}$/*Sdc1*$^{-/-}$ mice suggests a difference in activation or stability of the cytokine.

The recruitment of CD8$^+$ cells depends on the expression of CXCL-10 (60). Interestingly, *Dcn*$^{-/-}$ lymphocytes stimulated with CXCL-10 and CD3ε show a reduced adhesion to endothelial cells in contrast to wild-type. One might speculate that *Dcn*$^{-/-}$ lymphocytes have a different adhesion receptor profile compared with wild type, as reported for *Dcn*$^{-/-}$ fibroblasts (42, 59). The CD3ε stimulation may lead to changes on the cell surface that result in a decrease of activity. This might explain why the *Dcn*$^{-/-}$ leukocytes do not undergo transmigration (26). As *Ccl2* mRNA is up-regulated in inflamed *Dcn*$^{-/-}$ ears (26), it is unlikely that this chemokine may play a role in the reduced diapedesis in *Dcn*$^{-/-}$ mice. However, this might explain the increased recruitment of lymphocytes and increased amount of adhesion molecules. Collectively, our results suggest that decorin deficiency influences adhesion ligand expression via modulation of cytokine signaling in endothelial cells.

In bEnd.3 cells, TNF-α stimulation in the presence of DS decorin or protein core treatment leads to a significant inhibition of CCL2 in contrast to TNF-α alone. This might explain why *Dcn*$^{-/-}$ mice express increased levels of CCL2 promoting the recruitment of leukocytes. IFN-γ treatment of bEnd.3 cells shows an up-regulation of CXCL10 without any influence of decorin. Furthermore, the synthesis of CXCL-10 *in vitro* is dependent on the specific GAG chain as DS, but not chondroitin sulfate, is necessary for efficient IFN-γ signaling and induction of CXCL-10 in bEnd.3 cells. For chondroitin sulfate and heparin, it has been shown before that these GAGs can inhibit the binding of IFN-γ to COLO-205 cells (61). This would explain that the reduced amount of CD8$^+$ cells produced less IFN-γ and that the second influence is the lack of decorin and DS that prevents the synthesis of CXCL-10 by endothelial cells for the first 24 h (38). In fibroblasts derived from *Dcn*$^{-/-}$ or wild-type mice, decorin, but not the decorin core, induced an increase in CXCL-10 expression after IFN-γ treatment. CS4S and CS6S show no effect. In contrast, in DS an ~50% epimerization isolated from skin fibroblast-derived decorin (40) increases CXCL-10 expression after IFN-γ treatment exclusively in *Dcn*$^{-/-}$ fibroblasts. CXCL-10 is also affected *in vivo*. The loss of the DS proteoglycan decorin in the skin leads to a significantly reduced amount CXCL-10 protein during 24 h of DTH. The amount synthesized in *Dcn*$^{-/-}$ ears can be explained by the fact that in skin TNF-α is inducing the chemokine (10), too.

It is well established that GAGs can stabilize chemokines and cytokines (62, 63). In this study, we observed that decorin also enhances IFN-γ stability, which could explain, at least in part, the increased IFN-γ levels and edema formation in wild-type mice. Proteoglycans can influence not only the stability but also potentiate signaling events. There are two major signaling pathways induced by IFN-γ, NF-κB, and STAT-1 (64). In contrast to the role of decorin in septic inflammation (20), NF-κB signaling is not affected in our model. However, because of increased stability of IFN-γ, the levels of STAT-1, a key transcription factor involved in IFN-γ signaling (65), were increased in wild-type cells. Of note, interference with STAT-1 function has previously been shown to reduce DTH responses in an experimental model of arthritis and in contact hypersensitivity, underscoring the pre-clinical relevance of our findings (66, 67).

In summary, our data indicate a novel role for decorin and its DS chain in orchestrating the allergic inflammatory response (Fig. 6). Decorin-induced stabilization of IFN-γ results in increased activation of STAT-1, a transcription factor regulating the expression of a variety of inflammatory factors. In turn, the absence of decorin leads to a deregulation of cytokine expression, resulting in altered leukocyte adhesion receptor expression and defects in leukocyte diapedesis. The anti-adhesive function of decorin, deregulated expression of CXCL-11 and iNOS2, as identified in the TaqMan low density array analysis (Table 1), and stability of additional cytokines may have further promoted the anti-inflammatory phenotype. Our data may stimulate new research on nonsteroidal anti-inflammatory treatment approaches of contact hypersensitivity responses, marking decorin and its DS chain as attractive novel therapeutic targets.

Acknowledgments—We thank Margret Bahl, Anne Forsberg, and Birgit Pers for their expert technical assistance and Dr. Larry Fisher for the generous gift of decorin antiserum. We thank Prof. Dr. Lydia Sorokin for the opportunity to access the FACScalibur and the fluorescence microscope.

REFERENCES

1. Grabbe, S., and Schwarz, T. (1998) Immunoregulatory mechanisms involved in elicitation of allergic contact hypersensitivity. *Immunol. Today* **19,** 37–44
2. Kaplan, D. H., Igyártó, B. Z., and Gaspari, A. A. (2012) Early immune events in the induction of allergic contact dermatitis. *Nat. Rev. Immunol.* **12,** 114–124
3. Kish, D. D., Volokh, N., Baldwin, W. M., 3rd, and Fairchild, R. L. (2011) Hapten application to the skin induces an inflammatory program directing hapten-primed effector CD8 T cell interaction with hapten-presenting endothelial cells. *J. Immunol.* **186,** 2117–2126
4. Xu, H., Banerjee, A., Dilulio, N. A., and Fairchild, R. L. (1997) Development of effector CD8$^+$ T cells in contact hypersensitivity occurs independently of CD4$^+$ T cells. *J. Immunol.* **158,** 4721–4728
5. Wang, B., Fujisawa, H., Zhuang, L., Freed, I., Howell, B. G., Shahid, S., Shivji, G. M., Mak, T. W., and Sauder, D. N. (2000) CD4$^+$ Th1 and CD8$^+$ type 1 cytotoxic T cells both play a crucial role in the full development of contact hypersensitivity. *J. Immunol.* **165,** 6783–6790
6. Ahlfors, E. E., and Lyberg, T. (2010) Kinetics of local tissue and regional lymph node IL-2 and IFN-γ responses in experimental oral mucosa and skin contact sensitivity in mice. *Scand. J. Immunol.* **72,** 8–14
7. Engeman, T., Gorbachev, A. V., Kish, D. D., and Fairchild, R. L. (2004) The intensity of neutrophil infiltration controls the number of antigen-primed CD8 T cells recruited into cutaneous antigen challenge sites. *J. Leukocyte Biol.* **76,** 941–949
8. Norman, M. U., Hwang, J., Hulliger, S., Bonder, C. S., Yamanouchi, J., Santamaria, P., Kubes, P. (2008) Mast cells regulate the magnitude and the cytokine microenvironment of the contact hypersensitivity response. *Am. J. Pathol.* **172,** 1638–1649
9. Shibata, M., Sueki, H., Suzuki, H., Watanabe, H., Ohtaki, H., Shioda, S., Nakanishi-Ueda, T., Yasuhara, H., Sekikawa, K., and Iijima, M. (2005) Impaired contact hypersensitivity reaction and reduced production of

Downloaded from http://www.jbc.org/ at Istituto Superiore di Sanità on December 12, 2013

vascular endothelial growth factor in tumor necrosis factor-α gene-deficient mice. *J. Dermatol.* **32,** 523–533
10. Nakae, S., Komiyama, Y., Narumi, S., Sudo, K., Horai, R., Tagawa, Y., Sekikawa, K., Matsushima, K., Asano, M., and Iwakura, Y. (2003) IL-1-induced tumor necrosis factor-α elicits inflammatory cell infiltration in the skin by inducing IFN-γ-inducible protein 10 in the elicitation phase of the contact hypersensitivity response. *Int. Immunol.* **15,** 251–260
11. Itakura, A., Kikuchi, Y., Kouro, T., Ikutani, M., Takaki, S., Askenase, P. W., and Takatsu, K. (2006) Interleukin 5 plays an essential role in elicitation of contact sensitivity through dual effects on eosinophils and B-1 cells. *Int. Arch. Allergy Immunol.* **140,** 8–16
12. Hope, J. C., Campbell, F., and Hopkins, S. J. (2000) Deficiency of IL-2 or IL-6 reduces lymphocyte proliferation, but only IL-6 deficiency decreases the contact hypersensitivity response. *Eur. J. Immunol.* **30,** 197–203
13. Wang, L., Brown, J. R., Varki, A., and Esko, J. D. (2002) Heparin's anti-inflammatory effects require glucosamine 6-*O*-sulfation and are mediated by blockade of L- and P-selectins. *J. Clin. Invest.* **110,** 127–136
14. Ku, H. O., Jeong, S. H., Kang, H. G., Pyo, H. M., Cho, J. H., Son, S. W., Yun, S. M., and Ryu, D. Y. (2009) Gene expression profiles and pathways in skin inflammation induced by three different sensitizers and an irritant. *Toxicol. Lett.* **190,** 231–237
15. Anthoni, M., Fyhrquist-Vanni, N., Wolff, H., Alenius, H., and Lauerma, A. (2008) Transforming growth factor-β/Smad3 signalling regulates inflammatory responses in a murine model of contact hypersensitivity. *Br. J. Dermatol.* **159,** 546–554
16. Lehtimäki, S., Tillander, S., Puustinen, A., Matikainen, S., Nyman, T., Fyhrquist, N., Savinko, T., Majuri, M. L., Wolff, H., Alenius, H., and Lauerma, A. (2010) Absence of CCR4 exacerbates skin inflammation in an oxazolone-induced contact hypersensitivity model. *J. Invest. Dermatol.* **130,** 2743–2751
17. Kusumoto, M., Xu, B., Shi, M., Matsuyama, T., Aoyama, K., and Takeuchi, T. (2007) Expression of chemokine receptor CCR4 and its ligands (CCL17 and CCL22) in murine contact hypersensitivity. *J. Interferon Cytokine Res.* **27,** 901–910
18. Jin, H., Kumar, L., Mathias, C., Zurakowski, D., Oettgen, H., Gorelik, L., and Geha, R. (2009) Toll-like receptor 2 is important for the T(H)1 response to cutaneous sensitization. *J. Allergy Clin. Immunol.* **123,** 875–82.e1
19. Martin, S. F., Dudda, J. C., Bachtanian, E., Lembo, A., Liller, S., Dürr, C., Heimesaat, M. M., Bereswill, S., Fejer, G., Vassileva, R., Jakob, T., Freudenberg, N., Termeer, C. C., Johner, C., Galanos, C., and Freudenberg, M. A. (2008) Toll-like receptor and IL-12 signaling control susceptibility to contact hypersensitivity. *J. Exp. Med.* **205,** 2151–2162
20. Merline, R., Moreth, K., Beckmann, J., Nastase, M. V., Zeng-Brouwers, J., Tralhão, J. G., Lemarchand, P., Pfeilschifter, J., Schaefer, R. M., Iozzo, R. V., and Schaefer, L. (2011) Signaling by the matrix proteoglycan decorin controls inflammation and cancer through PDCD4 and microRNA-21. *Sci. Signal.* **4,** ra75
21. Cabello-Verrugio, C., Santander, C., Cofré, C., Acuña, M. J., Melo, F., and Brandan, E. (2012) The internal region leucine-rich repeat 6 of decorin interacts with low density lipoprotein receptor-related protein-1, modulates transforming growth factor (TGF)-β-dependent signaling, and inhibits TGF-β-dependent fibrotic response in skeletal muscles. *J. Biol. Chem.* **287,** 6773–6787
22. Schaefer, L., Macakova, K., Raslik, I., Micegova, M., Gröne, H. J., Schönherr, E., Robenek, H., Echtermeyer, F. G., Grässel, S., Bruckner, P., Schaefer, R. M., Iozzo, R. V., and Kresse, H. (2002) Absence of decorin adversely influences tubulointerstitial fibrosis of the obstructed kidney by enhanced apoptosis and increased inflammatory reaction. *Am. J. Pathol.* **160,** 1181–1191
23. Comalada, M., Cardó, M., Xaus, J., Valledor, A. F., Lloberas, J., Ventura, F., and Celada, A. (2003) Decorin reverses the repressive effect of autocrine-produced TGF-β on mouse macrophage activation. *J. Immunol.* **170,** 4450–4456
24. Tufvesson, E., and Westergren-Thorsson, G. (2002) Tumour necrosis factor-α interacts with biglycan and decorin. *FEBS Lett.* **530,** 124–128
25. Marchica, C. L., Pinelli, V., Borges, M., Zummer, J., Narayanan, V., Iozzo, R. V., and Ludwig, M. S. (2011) A role for decorin in a murine model of allergen-induced asthma. *Am. J. Physiol. Lung Cell. Mol. Physiol.* **300,** L863–L873
26. Seidler, D. G., Mohamed, N. A., Bocian, C., Stadtmann, A., Hermann, S., Schäfers, K., Schäfers, M., Iozzo, R. V., Zarbock, A., and Götte, M. (2011) The role for decorin in delayed-type hypersensitivity. *J. Immunol.* **187,** 6108–6119
27. Götte, M., (2003) Syndecans in inflammation. *FASEB J.* **17,** 575–591
28. Seidler, D. G., and Dreier, R. (2008) Decorin and its galactosaminoglycan chain: extracellular regulator of cellular function? *IUBMB. Life* **60,** 729–733
29. Wang, B., Feliciani, C., Howell, B. G., Freed, I., Cai, Q., Watanabe, H., and Sauder, D. N. (2002) Contribution of Langerhans cell-derived IL-18 to contact hypersensitivity. *J. Immunol.* **168,** 3303–3308
30. Wang, L., Fuster, M., Sriramarao, P., and Esko, J. D. (2005) Endothelial heparan sulfate deficiency impairs L-selectin- and chemokine-mediated neutrophil trafficking during inflammatory responses. *Nat. Immunol.* **6,** 902–910
31. Edovitsky, E., Lerner, I., Zcharia, E., Peretz, T., Vlodavsky, I., and Elkin, M. (2006) Role of endothelial heparanase in delayed-type hypersensitivity. *Blood* **107,** 3609–3616
32. Kharabi Masouleh, B., Ten Dam, G. B., Wild, M. K., Seelige, R., van der Vlag, J., Rops, A. L., Echtermeyer, F. G., Vestweber, D., van Kuppevelt, T. H., Kiesel, L., and Götte, M. (2009) Role of the heparan sulfate proteoglycan syndecan-1 (CD138) in delayed-type hypersensitivity. *J. Immunol.* **182,** 4985–4993
33. Schaefer, L., and Iozzo, R. V. (2012) Small leucine-rich proteoglycans, at the crossroad of cancer growth and inflammation. *Curr. Opin. Genet. Dev.* **22,** 56–57
34. Lee, S., Bowrin, K., Hamad, A. R., and Chakravarti, S. (2009) Extracellular matrix lumican deposited on the surface of neutrophils promotes migration by binding to β2 integrin. *J. Biol. Chem.* **284,** 23662–23669
35. Schaefer, L., Babelova, A., Kiss, E., Hausser, H. J., Baliova, M., Krzyzankova, M., Marsche, G., Young, M. F., Mihalik, D., Götte, M., Malle, E., Schaefer, R. M., and Gröne, H. J. (2005) The matrix component biglycan is proinflammatory and signals through Toll-like receptors 4 and 2 in macrophages. *J. Clin. Invest.* **115,** 2223–2233
36. Babelova, A., Moreth, K., Tsalastra-Greul, W., Zeng-Brouwers, J., Eickelberg, O., Young, M. F., Bruckner, P., Pfeilschifter, J., Schaefer, R. M., Gröne, H. J., and Schaefer, L. (2009) Biglycan, a danger signal that activates the NLRP3 inflammasome via toll-like and P2X receptors. *J. Biol. Chem.* **284,** 24035–24048
37. Götte, M., Kresse, H., and Hausser, H. (1995) Endocytosis of decorin by bovine aortic endothelial cells. *Eur. J. Cell Biol.* **66,** 226–233
38. Brooks, B., Briggs, D. M., Eastmond, N. C., Fernig, D. G., and Coleman, J. W. (2000) Presentation of IFN-γ to nitric oxide-producing cells: a novel function for mast cells. *J. Immunol.* **164,** 573–579
39. Penc, S. F., Pomahac, B., Eriksson, E., Detmar, M., and Gallo, R. L. (1999) Dermatan sulfate activates nuclear factor-κB and induces endothelial and circulating intercellular adhesion molecule-1. *J. Clin. Invest.* **103,** 1329–1335
40. Seidler, D. G., Faiyaz-Ul-Haque, M., Hansen, U., Yip, G. W., Zaidi, S. H., Teebi, A. S., Kiesel, L., and Götte, M. (2006) Defective glycosylation of decorin and biglycan, altered collagen structure, and abnormal phenotype of the skin fibroblasts of an Ehlers-Danlos syndrome patient carrying the novel Arg270Cys substitution in galactosyltransferase I (β4GalT-7). *J. Mol. Med.* **84,** 583–594
41. Ramamurthy, P., Hocking, A. M., and McQuillan, D. J. (1996) Recombinant decorin glycoforms. Purification and structure. *J. Biol. Chem.* **271,** 19578–19584
42. Jungmann, O., Nikolovska, K., Stock, C., Schulz, J. N., Eckes, B., Riethmüller, C., Owens, R. T., Iozzo, R. V., and Seidler, D. G. (2012) The dermatan sulfate proteoglycan decorin modulates α2β1 integrin and the vimentin intermediate filament system during collagen synthesis. *PLoS One* **7,** e50809
43. Danielson, K. G., Baribault, H., Holmes, D. F., Graham, H., Kadler, K. E., and Iozzo, R. V. (1997) Targeted disruption of decorin leads to abnormal collagen fibril morphology and skin fragility. *J. Cell Biol.* **136,** 729–743
44. Seidler, D. G., Schaefer, L., Robenek, H., Iozzo, R. V., Kresse, H., and

Downloaded from http://www.jbc.org/ at Istituto Superiore di Sanità on December 12, 2013

Schönherr, E. (2005) A physiologic three-dimensional cell culture system to investigate the role of decorin in matrix organisation and cell survival. *Biochem. Biophys. Res. Commun.* **332,** 1162–1170
45. Rühland, C., Schönherr, E., Robenek, H., Hansen, U., Iozzo, R. V., Bruckner, P., and Seidler, D. G. (2007) The glycosaminoglycan chain of decorin plays an important role in collagen fibril formation at the early stages of fibrillogenesis. *FEBS J.* **274,** 4246–4255
46. Montesano, R., Pepper, M. S., Möhle-Steinlein, U., Risau, W., Wagner, E. F., and Orci, L. (1990) Increased proteolytic activity is responsible for the aberrant morphogenetic behavior of endothelial cells expressing the middle T oncogene. *Cell* **62,** 435–445
47. Portoles, P., Rojo, J., Golby, A., Bonneville, M., Gromkowski, S., Greenbaum, L., Janeway, C. A., Jr., Murphy, D. B., and Bottomly, K. (1989) Monoclonal antibodies to murine CD3ϵ define distinct epitopes, one of which may interact with CD4 during T cell activation. *J. Immunol.* **142,** 4169–4175
48. Taub, D. D., Lloyd, A. R., Conlon, K., Wang, J. M., Ortaldo, J. R., Harada, A., Matsushima, K., Kelvin, D. J., and Oppenheim, J. J. (1993) Recombinant human interferon-inducible protein 10 is a chemoattractant for human monocytes and T lymphocytes and promotes T cell adhesion to endothelial cells. *J. Exp. Med.* **177,** 1809–1814
49. Floer, M., Götte, M., Wild, M. K., Heidemann, J., Gassar, E. S., Domschke, W., Kiesel, L., Luegering, A., and Kucharzik, T. (2010) Enoxaparin improves the course of dextran sodium sulfate-induced colitis in syndecan-1-deficient mice. *Am. J. Pathol.* **176,** 146–157
50. Zamfir, A. D., Flangea, C., Sisu, E., Serb, A. F., Dinca, N., Bruckner, P., and Seidler, D. G. (2009) Analysis of novel over- and under-sulfated glycosaminoglycan sequences by enzyme cleavage and multiple stage MS. *Proteomics.* **9,** 3435–3444
51. Flacher, V., Douillard, P., Aït-Yahia, S., Stoitzner, P., Clair-Moninot, V., Romani, N., and Saeland, S. (2008) Expression of langerin/CD207 reveals dendritic cell heterogeneity between inbred mouse strains. *Immunology* **123,** 339–347
52. Livak, K. J., and Schmittgen, T. D. (2001) Analysis of relative gene expression data using real-time quantitative PCR and the $2(-\Delta\Delta C(T))$ method. *Methods* **25,** 402–408
53. Goka A. K., and Farthing, M. J. (1987) The use of 3,3′,5,5′-tetramethylbenzidine as a peroxidase substrate in microplate enzyme-linked immunosorbent assay. *J. Immunoassay* **8,** 29–41
54. Thomson, J. A., Troutt, A. B., and Kelso, A. (1993) Contact sensitization to oxazolone: involvement of both interferon-γ and interleukin-4 in oxazolone-specific Ig and T-cell responses. *Immunology* **78,** 185–192
55. Shetty, S., Weston, C. J., Oo, Y. H., Westerlund, N., Stamataki, Z., Youster, J., Hubscher, S. G., Salmi, M., Jalkanen, S., Lalor, P. F., and Adams, D. H. (2011) Common lymphatic endothelial and vascular endothelial receptor-1 mediates the transmigration of regulatory T cells across human hepatic sinusoidal endothelium. *J. Immunol.* **186,** 4147–4155
56. Goldoni, S., Humphries, A., Nyström, A., Sattar, S., Owens, R. T., McQuillan, D. J., Ireton, K., and Iozzo, R. V. (2009) Decorin is a novel antagonistic ligand of the Met receptor. *J. Cell Biol.* **185,** 743–754
57. Buraschi, S., Pal, N., Tyler-Rubinstein, N., Owens, R. T., Neill, T., and Iozzo, R. V. (2010) Decorin antagonizes Met receptor activity and down-regulates β-catenin and Myc levels. *J. Biol. Chem.* **285,** 42075–42085
58. Neill, T., Painter, H., Buraschi, S., Owens, R. T., Lisanti, M. P., Schaefer, L., and Iozzo, R. V. (2012) Decorin antagonizes the angiogenic network: concurrent inhibition of Met, HIF-1α, and VEGFA and induction of thrombospondin-1 and TIMP-3. *J. Biol. Chem.* **287,** 5492–5506
59. Ferdous, Z., Peterson, S. B., Tseng, H., Anderson, D. K., Iozzo, R. V., and Grande-Allen, K. J. (2010) A role for decorin in controlling proliferation, adhesion, and migration of murine embryonic fibroblasts. *J. Biomed. Mater. Res. A* **93,** 419–428
60. Dufour, J. H., Dziejman, M., Liu, M. T., Leung, J. H., Lane, T. E., and Luster, A. D. (2002) IFN-γ-inducible protein 10 (IP-10; CXCL10)-deficient mice reveal a role for IP-10 in effector T cell generation and trafficking. *J. Immunol.* **168,** 3195–3204
61. Fernandez-Botran, R., Yan, J., and Justus, D. E. (1999) Binding of interferon γ by glycosaminoglycans: a strategy for localization and/or inhibition of its activity. *Cytokine* **11,** 313–325
62. Salek-Ardakani, S., Arrand, J. R., Shaw, D., and Mackett, M. (2000) Heparin and heparan sulfate bind interleukin-10 and modulate its activity. *Blood* **96,** 1879–1888
63. Reeves, E. P., Williamson, M., Byrne, B., Bergin, D. A., Smith, S. G., Greally, P., O'Kennedy, R., O'Neill, S. J., and McElvaney, N. G. (2010) IL-8 dictates glycosaminoglycan binding and stability of IL-18 in cystic fibrosis. *J. Immunol.* **184,** 1642–1652
64. Tamassia, N., Calzetti, F., Ear, T., Cloutier, A., Gasperini, S., Bazzoni, F., McDonald, P. P., and Cassatella, M. A. (2007) Molecular mechanisms underlying the synergistic induction of CXCL10 by LPS and IFN-γ in human neutrophils. *Eur. J. Immunol.* **37,** 2627–2634
65. Yuan, C., Qi, J., Zhao, X., and Gao, C. (2012) Smurf1 protein negatively regulates interferon-γ signaling through promoting STAT1 protein ubiquitination and degradation. *J. Biol. Chem.* **287,** 17006–17015
66. Hückel, M., Schurigt, U., Wagner, A. H., Stöckigt, R., Petrow, P. K., Thoss, K., Gajda, M., Henzgen, S., Hecker, M., and Bräuer, R. (2006) Attenuation of murine antigen-induced arthritis by treatment with a decoy oligodeoxynucleotide inhibiting signal transducer and activator of transcription-1 (STAT-1). *Arthritis Res. Ther.* **8,** R17
67. Yin, Y., Sun, Y., Gu, L., Zheng, W., Gong, F., Wu, X., Shen, Y., and Xu, Q. (2011) Jaceosidin inhibits contact hypersensitivity in mice via down-regulating IFN-γ/STAT1/T-bet signaling in T cells. *Eur. J. Pharmacol.* **651,** 205–211

Downloaded from http://www.jbc.org/ at Istituto Superiore di Sanità on December 12, 2013

Bocian et al.,

Supplemental Material:

Supplement Figure 1:

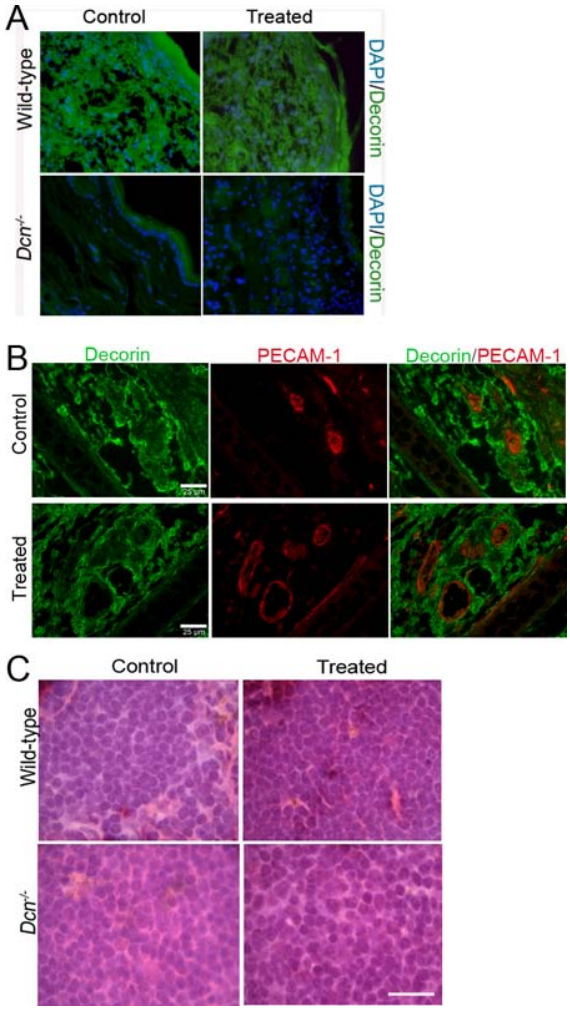

Supp. Figure 1: Characterization of wild-type and *Dcn*$^{-/-}$ organs – (*A*) Decorin detection with a specific decorin antibody (LF113; a generous gift from Larry Fisher) in wild-type control and treated ears and the respective *Dcn*$^{-/-}$ to demonstrate that decorin is present in the dermis. (*B*) Is decorin expressed in blood vessels during DTH? A PECAM-1 (Dianova) (red) and decorin (green) co-staining of the wild-type ears showed that decorin is not detected in the blood vessels of wild-type treated ears (24h after DTH induction). (*C*) Histology of wild-type and *Dcn*$^{-/-}$ 8 weeks old lymph nodes. The pictures show representative areas of H&E staining of control and treated lymph nodes with no obvious differences. Bar = 50µm.

Supplement Figure 2:

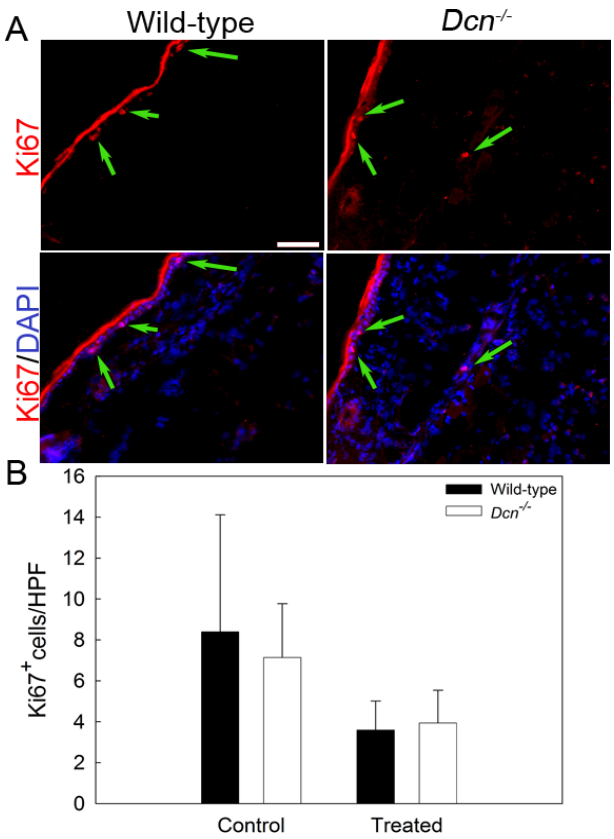

Supp. Figure 2: Ki67^{+} cells in ear tissue of *Dcn*$^{-/-}$ and wild-type mice 24 h after DTH induction. Frozen sections from untreated controls and oxazolone-treated ears of wild-type and *Dcn*$^{-/-}$ mice were prepared and stained for the proliferation marker Ki67. A representative immunofluorescence staining of treated ear tissue is displayed in figure *A* (bar = 50 µm). The upper panel shows a single staining for Ki67 (red), the lower panel is merged with a DAPI nuclei staining (blue). Ki67^{+} cells are marked with green arrows. Quantification (*B*) shows no alteration of Ki67^{+} cells in untreated or treated ear tissue of wild-type and *Dcn*$^{-/-}$ mice (n=3; p>0.6; mean±SD).

Supplement Figure 3:

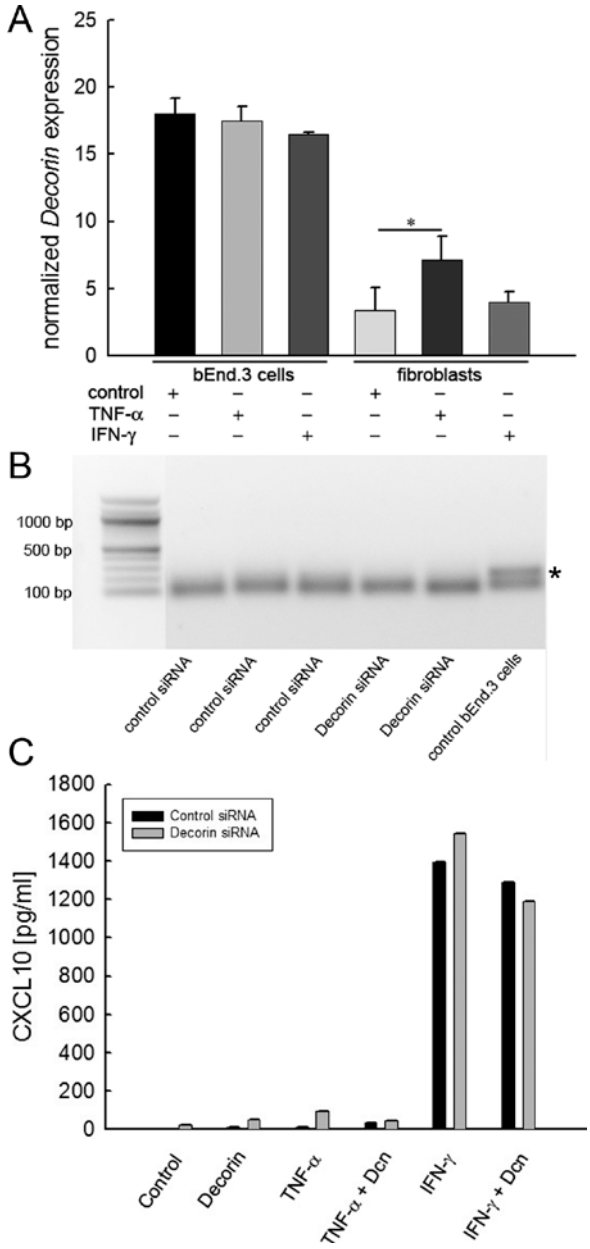

Suppl. Figure 3: Expression of decorin in bEnd.3 and fibroblasts cells and the influence on CXCL-10. bEnd.3 cells were cultured and treated with either TNF-α or IFN-γ followed by cDNA synthesis as described in Material & Methods. qRT-PCR for decorin was performed and Ct values are normalized to β-actin. The ΔCt values are shown mean±SD. (*A*) bEnd.3 cells express decorin mRNA under our culture conditions, but the expression is not influenced by treatment with either TNF-α or IFN-γ. Wild-type mouse fibroblasts express lower amount of decorin compared to bEnd.3 cells, which can be explained that cells were not confluent. Interestingly, TNF-α treatment of fibroblasts leads to a significant increase in decorin mRNA in contrast to IFN-γ which had no influence (TNF-α (2 independent experiments); control and IFN-γ (3 independent experiments; $p \leq 0.5$)). (*B*) bEnd.3 cells were transfected with siRNA for decorin. Knock-down of decorin was confirmed by RT-PCR. (*C*) CXCL-10 ELISA with bEnd.3 cells after decorin siRNA followed different treatments. The endogenous decorin, like the added decorin had no impact on CXCL-10 expression of bEnd.3 cells (n=3).

Supplement Figure 4:

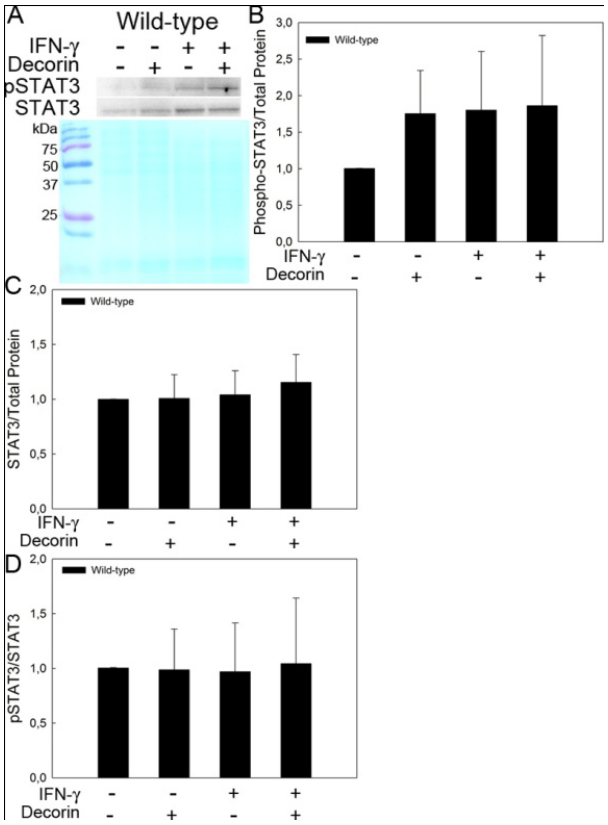

Supp. Figure 4: **STAT-3 expression of IFN-γ stimulated wild-type fibroblasts.** Figure *A* shows Western blot analysis for the phosphorylated and non-phosphorylated form of STAT-3. Quantifications show no evidence of an altered expression of pSTAT-3/STAT-3 (*B*), STAT-3(*C*) and pSTAT-3 (*D*) in wild-type fibroblasts (n=4; mean±SEM).

Supplement Figure 5:

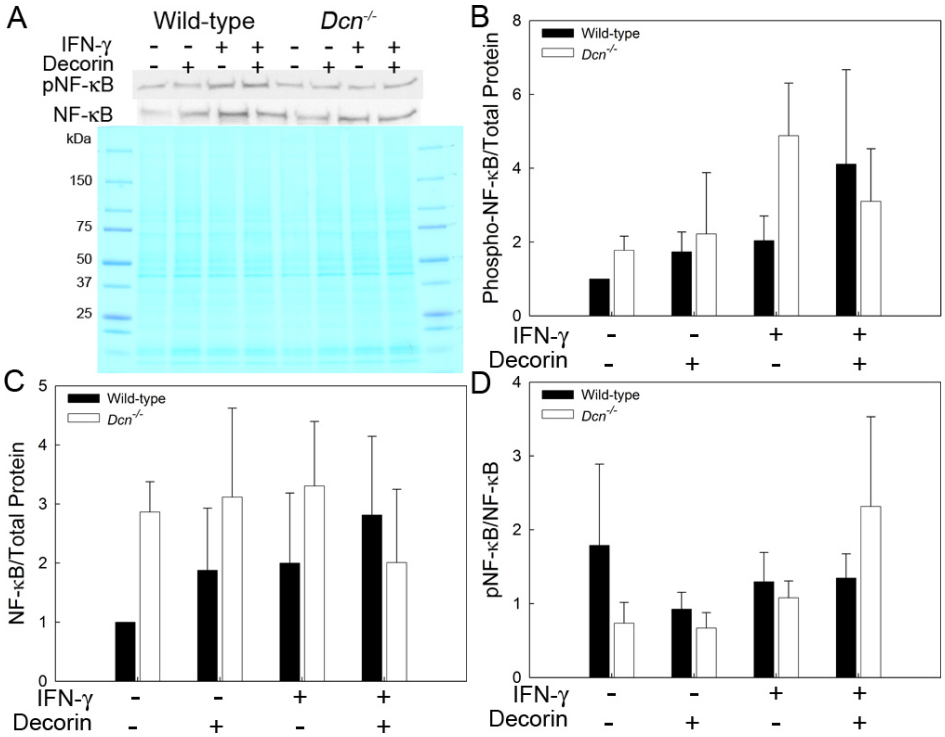

Supp. Figure 5: **NF-κB expression of IFN-γ stimulated wild-type or *Dcn*$^{-/-}$ fibroblasts is not altered by decorin.** Figure *A* shows Western blot analysis for the phosphorylated and non-phosphorylated form of NF-κB as well as a total protein stain. (*B-D*) Quantifications show no alteration of NF-κB or pNF-κB expression in fibroblasts of wild-type and *Dcn*$^{-/-}$ mice (n=4; mean ±SEM).